TECHNISCHE UNIVERSITÄT WIEN
Vienna University of Technology

Master thesis

Computer simulation of volume changes during phase transformation in Al-Si, Al-Cu, and Al-Mg-Si alloys

Executed with the purpose of attaining the academical degree of Master of Science

under the direction of

Univ.Prof. Dipl.-Ing. Dr.techn. Ernst Kozeschnik

at the

Institute for Materials Science and Material Technology

Submitted to the Technical University Vienna

Department for Mechanical Engineering and Science of Management

by

Olivier NODIN

Vienna, August 1st, 2010

A Marie

“ Chaque mot de mon chant c’est de toi qu’il venait”

(L. Aragon)

Acknowledgements

First of all, I would like to thank Pr. Kozeschnik for having given me the opportunity to fulfil this master thesis at the Institute for material science and technology and having welcomed me in this institute.

This work was carried out under the supervision of Mr. Ahmad Falahati, PhD. I thank him for his help and addressability during this work. He answered my questions, and was present to advice me and lead this work during the summer term. He also read again and corrected with attention and precision the first issues of this work.

I would like also to thank my colleagues and fellow students of the institute for their help and the opinion sharing. It is very precious and important to discuss some results and share ideas. It has been an important help to carry out this work. Thank you Mohammad, Hamid, Peter, Erwin, Piotr. I would like to thank especially Hamid, Manoj, and Claire for comparison of results, opinion sharing and ideas. I will not forget to thank Mr. Zaruba, Mrs. Knoblich, Mr. Zellhofer, and Mr. Kaminski for their help and their advices for preparing samples and working with the different devices. Their patience, their experience and their advices were important for me.

This project could be led out with the kind financial support of the Institute for Material science and Technologies.

Finally, I would also like to thank my friends Alexandre, Jean and Emmanuel for their presence and ideas. This work is dedicated to my beloved Marie. She always supported and encouraged me, especially in rough times. Through her presence, she contributed actively to the achievement of this work.

Abstract

In the last decades, aluminium alloys have been increasingly used in industries. In car industries, they are used for the realisation of light weight panels for instance. Due to their properties, aluminium alloys are very interesting materials. One of most interesting property of some aluminium alloys is the precipitation hardening. Aluminium alloys of the 2xxx (Al-Cu-(Mg)), 6xxx (Al-Mg-Si-(Cu)) and 7xxx (Al-Zn-Mg) series develop precipitates when they are submitted to a suitable heat treatment. Some of these precipitates strongly improve the mechanical properties of these alloys.

Even if this process is well-known, observed and used in industrial heat treatment since a long time, many things regarding the nucleation, growth, influence of these precipitates on thermo-mechanical behaviour remain unclear and controversial. Among the testing methods that are used to inquire the precipitation process in aluminium alloys during artificial ageing, DSC and TMA are very popular. In the last years, progress in simulation allowed developing computational tools relying on thermodynamics computation.

Through comparison between simulations and experiments, we expect to get interesting information on the precipitation process in aluminium alloys. The question of the volume changes is especially interesting because volume changes during heating up can be correlated to expansion of the matrix due to temperature plus precipitations and dissolution of phases with different molar volumes. This allows detecting the formation and checking kinetics of the precipitates.

This work aims to model and simulate the volume changes in alloys during heat treatments. It relies on literature in order to collect data on the various precipitates and their structure, dilatometry experiments and thermo-kinetics simulation. It highlights how volume changes can be modelled using the MatCalc software and how the model can be evaluated by comparing the experiments with simulations.

The focus is on three different systems. Al-Si binary system, precipitation hardenable Al-Cu and Al-Mg-Si systems. Additionally it contains a collection of some structural and molar volume of precipitates in Aluminium alloys for further development and refinement of volume change simulations.

Zusammenfassung

In den letzten Jahrzenten nahm die Verwendung von Aluminiumlegierungen in der Industrie an Häufigkeit deutlich zu. Beispielsweise werden solche Legierungen für Leichtbauelemente im Kfz-Bau verwendet. Aufgrund ihrer Eigenschaften, wie geringer spezifischer Masse, Korrosionsbeständigkeit, sowie Verarbeitungsfähigkeit, sind Aluminiumlegierungen von besonderem Interesse. Eine der interessantesten Eigenschaften ist die Ausscheidungshärtungsfähigeit bestimmter Legierungen. Aluminiumlegierungen der 2xxx (Al-Cu-(Mg)), 6xxx (Al-Mg-Si-(Cu)) und 7xxx (Al-Z-Mg) Serie entwickeln bei geeigneter Wärmebehandlung Ausscheidungen. Einige dieser Ausscheidungen verbessern deutlich die mechanischen Eigenschaften dieser Legierungen.

Obwohl dieser Prozess wohl bekannt und beschrieben ist und in der industriellen Wärmebehandlung seit längerer Zeit angewendet wird, bleiben viele Aspekte bezüglich Nukleation, Wachstum und die Einflüsse dieser Ausscheidungen auf das thermomechanische Verhalten unklar. Unter den heutzutage populärsten Methoden zur Untersuchung des Ausscheidungsprozesses von Aluminiumlegierungen bei künstlicher Alterung gehören die dynamische Differenzkalorimetrie, sowie die Dilatometrie. In den letzten Jahren haben Fortschritte in der Modellbildung und der Simulation der Legierungen zur Entwicklung neuer Computerprogramme geführt, um die Eigenschaften der Legierungen aus thermodynamischer Sicht vorhersagen zu können.

Durch Vergleich zwischen Simulationen und Experimenten erwarten wir interessante Informationen über den Ausscheidungsprozess in Aluminiumlegierungen. Die Frage der Volumsänderungen ist besonders interessant, da die Volumsänderungen während des Aufwärmens mit der Expansion der Matrix aufgrund der Temperatur und der Ausscheidungen, sowie der Auflösung der Phasen bei unterschiedlichen molaren Volumen der Ausscheidungen korreliert werden können. Dies erlaubt das Erkennen der Bildung und das Überprüfen der Kinetik der Ausscheidungen.

Ziel der vorliegenden Arbeit ist die Modellierung und Simulation der Volumsänderungen einiger Aluminiumlegierungen während der Wärmebehandlung. Die Arbeit basiert auf einer Literaturrecherche, mit dem Ziel, Daten über Ausscheidungen und deren Strukturen zu sammeln, dilatometrischen Experimenten, sowie thermokinetischen Simulation. Die Arbeit beschäftigt sich mit der Frage, wie Volumsänderungen durch MatCalc-Berechnungen modelliert werden können und welche Schlüsse aus dem Vergleich dieser Modelle mit Experimenten gezogen werden können.

Der Fokus richtet sich auf drei unterschiedliche Legierungssysteme: Das Al-Si-System, Ausscheidungshärtbare Al-Cu und Al-Mg-Si Systeme. Weiterst beinhaltet die Arbeit eine Sammlung von molaren Volumen von unterschiedlichen Ausscheidungen für die weitere Entwicklung und Verbesserung der Volumsänderungssimulationen.

Table of Content

1. Introduction

Since the late years of the 19th century, aluminium alloys are industrially used. Due to good mechanical properties, corrosion resistance and very low specific weight, aluminium has become a very popular and often used material.

In the last two decades, automotive industry started to get interested in aluminium alloys. In the last few years they have attracted transportation industrial attention, not only because of their light weight contributing to more economical fuel consumption but also because of reducing air pollution and accomplishing the restricted new environmental laws. Nowadays aluminium alloys are being increasingly used for car panels. Other industries increasingly use aluminium alloys and this material can now be found in production of sports, aircraft and in construction industries.

The interesting property of heat treatable aluminium alloys is that by using alloying elements and specific heat treatments, hardness and strength of aluminium alloys can be improved. This hardening will be relied on the formation of precipitates in the aluminium microstructure.

In order to get a higher hardening, the composition of the alloy and the heat treatment can be adapted. The size, the number density and the distribution of precipitates will affect the hardening behaviour. In fact, precipitation process is complex and it must be underlined that any change in composition, heat treatment, working conditions and ageing procedure will affect the precipitation hardening behaviour.

In order to understand better what is happening at microscopic scale and to be able to relate it to the behaviour and mechanical properties at macroscopic scale, many studies have been led out in the last decades. Initially, they all relied on experimental observations and measurements. However, in the last years, due to improvement in computational tools, it has become possible to describe thermodynamically and geometrically the precipitates, even the metastable precipitates. This has opened new possibilities, in addition or parallel to experiments, to explain microstructural evolutions by using simulation and/or computational tools.

From another point of view, as many facts related to metastable phases remain still unclear, there exists a challenge for computational tools to provide more precise models and kinetic parameters not only for better understanding of microscopic evolution but also more precise prediction of material behaviour.

2. Objectives

Computer assisted modelling and simulation are new tools that can be used complementary to experiments for a better understanding of microscopic evolution during heat treatments. The aim and the motivation of this work were to inquire the possibility to model the volume changes in aluminium alloys during heat treatment using the program MatCalc[1].

First of all, structure data for different precipitates was collected, and density, temperature dependence and if necessary composition dependence of densities was computed for the phases which can appear in different aluminium alloy systems.

Then, experimental data which is a base for comparing simulation results and experiments was collected, either in literature or through achievement of experiments. DSC and TMA experiments were carried out for one single heat treatment. Several heating rates were used during these experiments and the results were processed in order to support the adjustment of modelling parameters.

Eventually, the developed physical database was tried and the MatCalc computation for simulation of volume changes. In the scope of the working group's activities, this modelling focused on three different alloys. Coefficient of Thermal Expansion (CTE) and heat flow predictions by MatCalc were compared with the experiments and with some simple ad-hoc models which were developed in the scope of this study.

This work is considered as a first step in the direction of modelling the volume changes of aluminium alloys, using thermo-kinetic computation software MatCalc. Simulated values of instantaneous CTE during heat treatments which include and show the direct effect of precipitations and microstructural evolution will be compared with experimental results and will be discussed.

1 Software available on http://www.matcalc.at

3. State of arts

3.1. Generalities about aluminium

Aluminium is the third most common element on the Earth crust after oxygen and silicon. It is estimated to be about 8% of it. Due to its high reactivity with oxygen, it is available as aluminium oxide, with the composition Al_2O_3. The difficulty to get pure aluminium was a reason for small amount of use of this metal until the end of the 19^{th} century. As a chemical process was developed to get pure aluminium from this oxide, aluminium started to be used industrially.

Aluminium has several advantages: Its specific mass, about 2700 kg/m^3, is low in comparison to other metals and alloys. For instance, pure aluminium has a specific mass which is about one third of the one of iron. Another interesting property is the possibility to improve aluminium's mechanical properties (especially strength and hardness) with alloying and suitable heat treatment.

Although aluminium is commonly used in the packaging and structure industries, it started to be increasingly used in other industries, especially car industry, in the scope of the weight reduction of the vehicles and has been used for some panels. Other industries interested in light weight design use Aluminium too.

Aluminium is known to have a FCC structure, with 4.04 Å lattice parameter at 298K. [1]. An atom of aluminium has a radius of 1.43 Å and the molar mass of aluminium is 26.98 g/mol.

3.1.1. Alloying systems

Pure Aluminium can be alloyed in order to improve its mechanical properties. There are two families of aluminium alloys: the cast alloys and the wrought alloys.

Many alloying elements can be found in aluminium alloys. The most commonly used alloying elements are silicon, magnesium, zinc and copper. Iron and manganese are also often available, but rather as impurities. Table 1 present the main alloying elements and their atomic radii and molar mass.

Table 1: Atomic radii and molar mass (data from [1])

Al	Mg	Si	Cu	Zn
R=1.43 Å	R=1.60 Å	R=1.32 Å	R=1.28 Å	R=1.38 Å
M=26.98 g/mol	M=24.31 g/mol	M=28.08 g/mol	M=63.55 g/mol	M=65.38 g/mol

All aluminium alloys are denoted by a number, depending on their alloying elements. For wrought aluminium alloys, this is a number of four digits. The first one indicates the main alloying elements.

Table 2: alloying systems for wrought alloys [2]

series	Main alloying elements
1xxx	Pure Aluminium
2xxx	Al-Cu-(Mg)
3xxx	Al-Mn
4xxx	Al-Si
5xxx	Al-Mg
6xxx	Al-Mg-Si-(Cu)
7xxx	Al-Zn-Mg
8xxx	Other alloying systems
9xxx	Not attributed

Under all alloying systems, the 2xxx (Al-Cu-(Mg)) alloys, the 6xxx (Al-Mg-Si-(Cu)) alloys and the 7xxxx (Al-Zn-Mg) alloys are heat treatable. It means that it is possible to improve their mechanical properties through a suitable heat treatment. [3]

3.1.2. Heat Treatments

Heat treatments allow improving the properties of alloys. For precipitation hardenable alloys, the aim is to control the size and distribution of precipitates. In fact, the hardness and yield strength will be all the better since the precipitates are more dispersed and numerous. In systems that allow forming several kinds of precipitates, some precipitates might have better hardening effect. Industrial heat treatments consist of several steps. They are introduced shortly here.

Homogenisation: Wrought aluminium alloys are often given a homogenisation heat treatment before extrusion or rolling and foundry alloys before age hardening. The main purpose is to remove particles and segregation gradients. The driving phenomenon is diffusion, which is a temperature dependent process. Thus, temperature must be high enough in order to have a sufficient diffusion at the same time must be chosen so that to avoid local melting. Homogenisation is generally performed at 70% to 85% of the melting temperature [2]. The sample are held in constant temperature for a long time (up to several days, depending on the samples size) in order to be homogenised. During the heating up of the sample, too high temperature must not be reached.

Solution heat treatment: means laying the sample at high temperature for a specific period of time in order to dissolve the maximum practical amounts of the soluble hardening alloying elements in solid solution. The temperature must be chosen between the solvus temperature of alloying elements and the melting point. This temperature is strongly dependant on the composition of the alloy. A too high temperature can lead to local melting which is undesirable.

Quenching: It is a sudden cooling down of specimen which normally is performed in cold (sometimes chilled) water. Some other quenching media can be used such as cool air or oil. It aims to freeze the micro-structure after the previous heat treatment. After solution treatment, quenching a sample, allows keeping a large

number of excess vacancy concentration (the so-called quenched-in vacancies) and solute atoms with higher concentration than the equilibrium one. It creates a supersaturated solid solution. The quenching rate is hard to estimate. It is strongly dependant on the quenching medium, the size and the geometry of the sample.

Natural ageing: consists in laying the sample after solution treatment and quenching at room temperature for some time. There are two main effects. First of all, there is a diminution of quenched-in vacancies with time. They will be trapped by some elements and clusters and recombine and annihilate. Second, the decomposition of the supersaturated solid solution also starts and early stages of precipitation are being formed.

Artificial ageing: is an ageing procedure at higher temperature than room temperature. Through increase of temperature, it is possible to enhance the precipitation kinetics and a given precipitation stage can be reached faster. Ageing temperature influences size, distribution and evolution stage of precipitation. Thus it influences the properties of the alloy.

Heat treatment is commonly denoted with a letter and a number. For instance a sample which has been solution treated, quenched and natural aged to a substantially stable condition will be said to be in the T4 state. An artificially aged sample will be called in the T6 state. If no ageing has been performed just after quenching, it is described as T4_fresh state. These denominations are standardised. It will not ve presented in details all different heat treatments that can exist. The aim is here to point out the one that are interesting in the scope of this study.

For aluminium alloys, a typical industrial heat treatment is T6. It includes solution treatment, quenching and then artificially ageing, normally at 100 to 200°C in order to get the most hardening effect. [4]

3.1.3. A historical overview

In 1906, the German physician Alfred Wilm discovered the age-hardening phenomenon while he was working on an Al-Cu-Mg alloy. He noticed accidentally a change in the mechanical properties, especially strength, of an alloy exposed to room temperature after high temperature heat treatment and quenching. Although he recognized the change, he could not explain it. This is the first observation of precipitation hardening in aluminium alloys.

This phenomenon was first explained in 1919 by a group of scientists, led by the British physician Mercia. They supposed that this phenomenon could be relied to some changes inside the aluminium matrix. In fact, as temperature decreases, equilibrium concentration of copper inside the aluminium lattice also decreases. From this observation, they proposed that the supersaturated solid solution formed after quenching could decompose into the aluminium lattice and some precipitate [3].

In 1938, two scientists, Andre Guinier [5] and Georges Preston observed independently using X-Ray scattering some changes inside the aluminium lattice after

ageing. This is the first observation of structural changes inside the aluminium matrix and this confirmed the assumption of Mercia.

After World War II, it was possible to observe directly the precipitates thanks to the progress in the filed of microscopy. As homage to the observation of Guinier and Preston who observed first the structural changes at microscopic scales (and thus confirmed the theory of precipitation processes) in an alloy after quenching, the early stages of precipitation are called Guinier-Preston Zones.

3.2. Aluminium-Silicon system

Aluminium-silicon system is a non age-hardenable alloy. In comparison to other aluminium alloys, it is one of the simplest binary system involving aluminium. The equilibrium precipitate is formed without any metastable intermediate phase. This system is well-known and well-described in literature. It has some practical application, for instance in automotive industry.

The partial phase diagram is presented on figure 1. The focus is the aluminium rich corner of the phase diagram, as this work deals with kinetics of Si precipitation of such alloys. The maximum solubility of silicon in the aluminium matrix is 1.65 wt.% at 577°C.

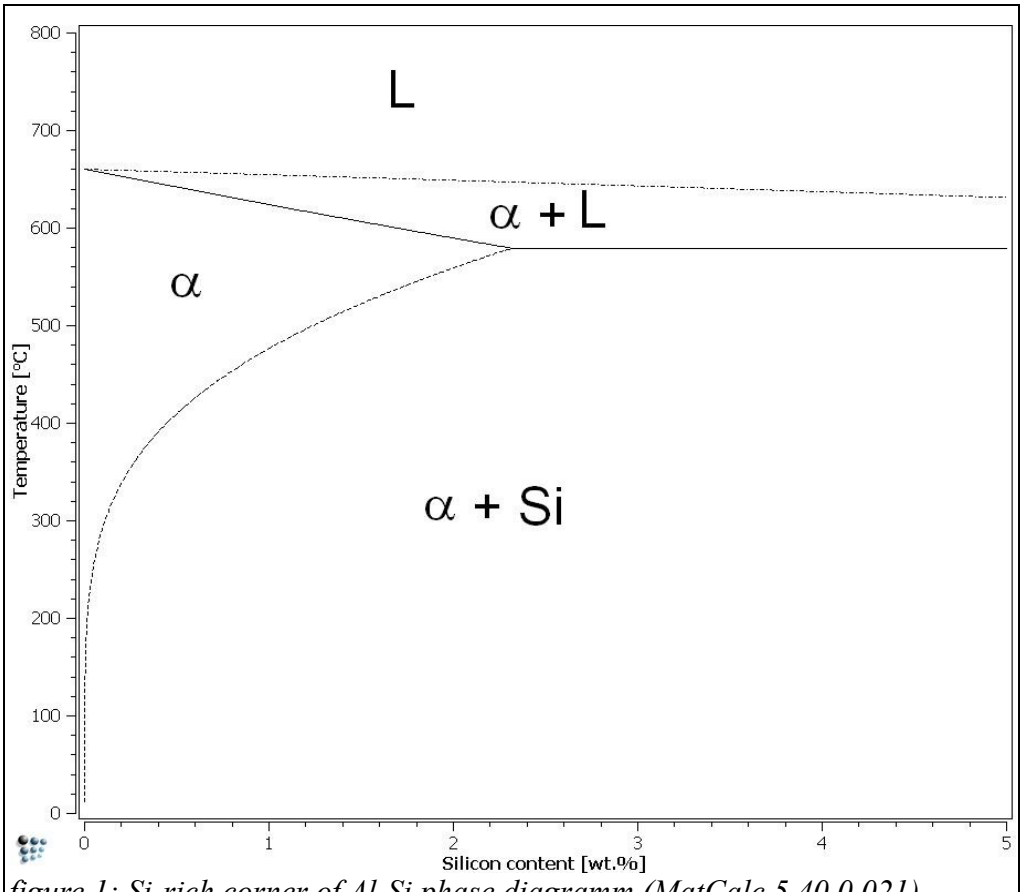

figure 1: Si-rich corner of Al-Si phase diagramm (MatCalc 5.40.0.021)

Equilibrium silicon precipitate has a diamond-like structure with 5.43Å of lattice parameter ([6, 7]). The group symmetry of such a precipitate is F_{d3m}

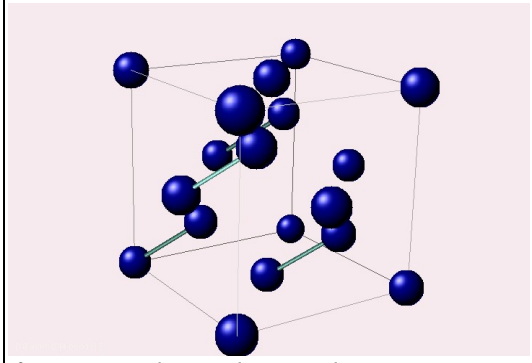

figure 2: Silicon diamond structure [8]

3.3. Aluminium Copper System

Aluminium-Copper alloys belong to the age-hardenable alloys. Historically, the first inquiries of precipitation hardening were led on this alloy.

The full phase diagram of the Al-Cu system is complex (see Figure 3) and many equilibrium phases can be formed according to the alloy's composition. For the scope of this study, only the Al-rich corner of the phase diagram is interesting. The maximum solubility of Copper atoms in the aluminium matrix is 5.65 wt.% at 548°C, which is the eutectic temperature [9].

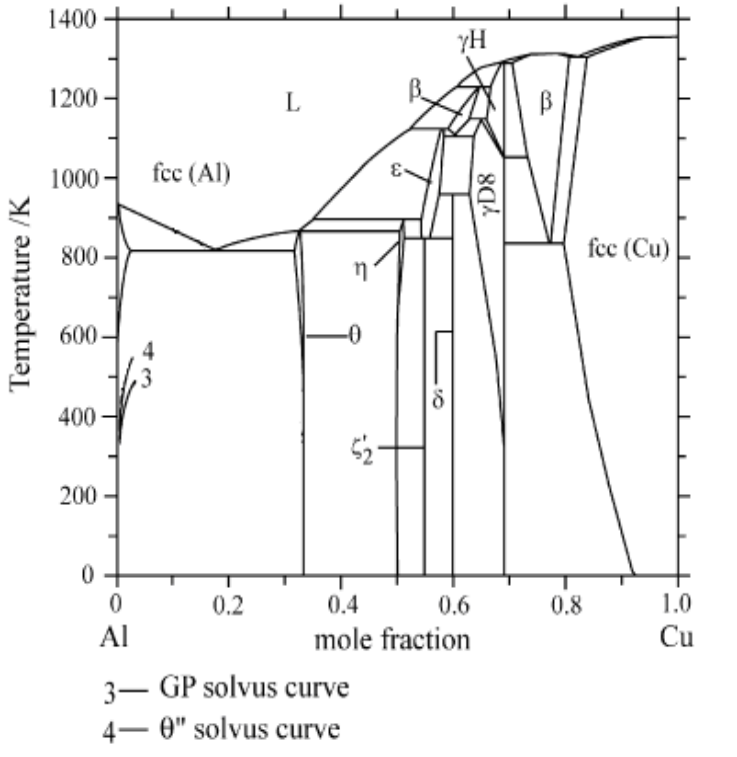

figure 3: The phase diagram of the Al-Cu system [10]

Precipitation process in Al-Cu alloys involves between 3 and 7 stages according to the different studies. The exact number of metastable phases, their composition, their structures and their growth kinetics are still controversial and topics of actual research [9]. In the next part the different precipitates of the most commonly admitted precipitation sequence (cf [11]) w ll be presented

$$\alpha_{ssss} \text{ -> GP-Zones -> } \theta'' \text{ -> } \theta' \text{ -> } \theta$$

3.3.1. Structure of the supersaturated solid solution

Supersaturated solid solution (SSSS) is obtained after solutionizing at high temperature (typically about 550°C) and quenching, which usually occurs in chilled or cold water. Due to this heat treatment, the matrix has a large excess of vacancy concentration. Copper atoms are randomly distributed inside the aluminium matrix and concentration of copper inside the matrix is over the equilibrium concentration. This is an unstable state, which is energetically not sustainable. The system tends to evolve from ssss toward an energetically more favourable state. Thus, there is an evolution of the system, which is governed by diffusion of the atoms and enhanced by excess vacancies and temperature.

At very early stages of precipitation some so-called quenched clusters of several atoms would be observed. Their structure and their morphology are monolayer Cu-rich plates are really close to the one of the GP-Zones, but they are much smaller: approximately a few nm in size [12]. Due to this property many authors do not consider them as an independent phase.

3.3.2. Guinier-Preston Zones (GP-Zones)

GP-Zones consist of platelets of copper atoms, with a 40 Å to 200 Å diameter, which are formed in substitution sites in aluminium lattice. The platelets are mono-layers of Cu atoms. They are formed parallel to the (100) planes of the aluminium matrix. [11, 13]. However the exact amounts of copper in the copper layers is still controversial and vary according to the studies between 40% and 100%. [10]

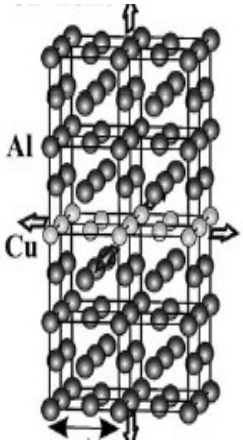

figure 4: The GP-Zones, crystal structure [9]

GP-Zones are widely admitted to be fully coherent with the aluminium matrix. Due to this coherence with the aluminium matrix and their small size, the GP-Zones are very difficult to inquire and to observe. [13]

In fact, the radius of the atoms of copper is much smaller than the radius of aluminium atoms (see table 1). Thus, the copper layer of the GP zones creates a field of strain and deforms the matrix. The lattice collapses in the neighbourhood of the GP-Zones. If this collapse is widely admitted, it has not been quantified with precision yet [9].

3.3.3. θ" precipitate

θ" precipitates are commonly seen as an arrangement of the GP-Zones in order to form a later phase of precipitation. It can be described as a formal stoichiometry $CuAl_3$, a periodic arrangement of aluminium and copper layers with the following stacking sequence $\{Cu, Al, Al, Al\}_N$. The lattice parameters of this precipitate are showed in figure 5. On this scheme, white spheres are copper atoms and black spheres aluminium atoms.

Some studies have also highlighted the presence of a GP-II phase which is intermediate between GP-Zones and θ" precipitates. This GP-II Zones were found to have a slightly different structure: two layers of copper separated by one layer of aluminium. [9].

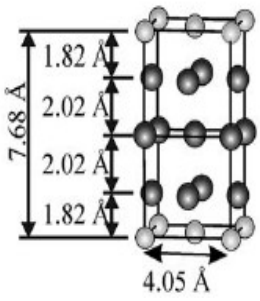

figure 5: The crystal structure of θ" precipitates [9]

Some recent studies highlighted that GP Zones and θ" precipitate are thermodynamically the same phase. The only different is a size and arrangement matter. [14]

3.3.4. θ' precipitate

θ' precipitate is a metastable stoichiometric precipitate with the composition Al_2Cu. The structure was found to be a tetragonal distortion of the fluorite structure. The distortion leads to a partial incoherent with the surrounding aluminium matrix along the c-axis of the tetragonal structure. The group symmetry is $I4_{mmm}$. The lattice parameters of this precipitate are showed on figure 6. The white spheres are copper atoms and black spheres aluminium atoms.

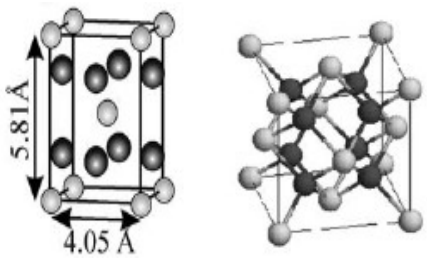

figure 6: The crystal structure of θ' precipitate [11, 13]

3.3.5. θ precipitate

θ precipitate is a fully incoherent precipitate. Its composition is the same as θ' precipitates. Among all the presented precipitates in Al-Cu system, this is the only stable one. Like the previous one, the structure of this precipitate is also a distortion of the fluorite structure, with the group symmetry $I4_{mcm}$ [11].

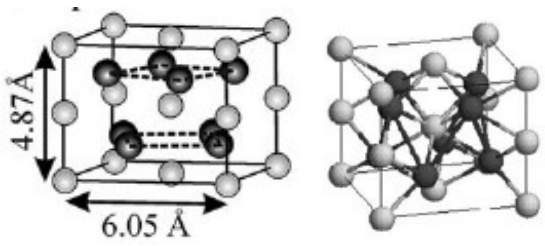

figure 7: The crystal structures of θ precipitate [11, 13]

3.3.6. Effect of Magnesium addition

In many alloys of the 2xxx-series, another alloying element, magnesium, can be present simultaneously with copper. It leads to modification of the precipitation sequence and formation of another kind of precipitate, the S-precipitate. This precipitate can be observed along with the θ precipitate as the stable pause in Al-Cu-Mg alloys. [15].

S precipitate has the composition $CuMgAl_2$. It has an orthorhombic structure with 16 atoms per unit cell and lattice parameters a=4.0 Å, b=9.23 Å and c=7.14 Å [16]. It has a sequence of metastable precursors. The precipitation sequences for the Al-Cu-Mg systems and their equilibrium precipitates are GP-Zones, S", S´, and S precipitates. [13]. Detail of all metastable precursors of the S precipitates is out of the scope of this study.

3.4. Aluminium-Magnesium-Silicon system

Al-Mg-Si alloys are an important group of alloys which are widely used in both cast and wrought form.. They are increasingly used for having very good mechanical and physical properties. They show also a good weldability and their hardness can be increased significantly after a suitable heat treatment. ([4, 17])

Precipitation process in this alloys family depends on the composition of the alloy and the Mg:Si ratio in this context is a very important parameter. Al-Mg-Si alloys trend to evolve at the end to stable phase Mg_2Si. There is a difference between so called balanced alloy where the stoichiometric ratio of the equilibrium phase is respected and so-called excess silicon alloys where there is too much silicon in regard to stoichiometric Mg_2Si. Excess Mg alloys also exists although they are not presented in this study. Whereas the excess Silicon alloys have some diamond-like silicon as stable phase, the Magnesium excess silicon would have other stable phases, coexisting with Mg_2Si precipitates [15].

The commercial Al-Mg-Si alloys have Iron and Manganese as impurities. These elements have no significant influence on the precipitation sequence and hardening behaviour of the alloys. They form some inter-metallic phases and consume some Si.

The excess amount of silicon and the available Mg_2Si amount can be computed. These values are often used to describe the Al-Mg-Si alloy. The following formulas (1) and (2) can be used to calculate these values [16]. The effect of Si picked up by Fe which makes intermetalic phases and reduces Si amount are also taken in to account by these formulas.

$$wt.\%(Mg_2Si) = wt.\%(Mg)\left(1+\frac{1}{1.73}\right) \approx 1.58\ wt.\%(Mg) \quad (1)$$

$$wt.\%(Si)_{excess} = wt.\%(Si) - \left(\frac{\text{wt.\%(Mg)}}{1.73} + \frac{\text{wt.\%(Fe)}}{4.0}\right) \quad (2)$$

Excess of silicon is not believed to alter the precipitation sequence. It promotes the formation of additional phases which are believed to contribute not significantly to hardening. Excess silicon changes the Mg/Si in clusters and affects number density, sizes and distribution of GP and ß” precipitates and it enhances the age hardening effects. This has an influence on the alloy hardening response. [18]

3.4.1. Precipitation sequence

Precipitation sequence in the aluminium-magnesium-silicon system is more complicated than in the previously introduced systems. Precipitation sequence is a controversial problem, specially early stage of precipitations. It is important to notice that change in composition, processing, heat treatment, ageing practice can lead to a change in the precipitation behaviour. [4, 19]

Generally speaking, precipitation is a progressive change from the energetically not favourable supersaturating solid solution to more stable precipitates. This process can also be considered as a decomposition of the supersaturated solid solution. This evolution occurs in several stages, which are commonly admitted to be the following: [20]

$$\alpha_{ssss} \text{ -> GP-Zones -> } \beta'' \text{ -> } \beta' \text{-> } \beta$$

However some other intermediate phases might be formed. Some authors give a slightly modified precipitation sequence which takes in account other metastable precipitates, which appearance depends on the alloy's composition [20]

α_{ssss} -> embryo clusters -> GP-Zones -> β" -> β' + B' + U1 + U2 -> β

The question whether the precipitates dissolve and resolve or rather evolve from one form to another is not cleared yet. Some precipitates which are given in a certain order in the previous precipitation sequence might however be observed at the same time. So a modified precipitation sequence might be introduced to take this in to account. [20]

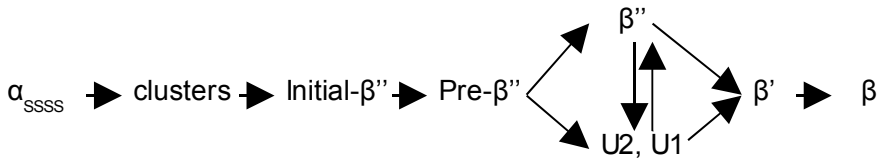

Some authors presented recently a modified version of the precipitation sequence. The metastable phase and their formation is a complex process which depends on different factors such as composition, strain, temperature etc.. From this point of view, the concept of a sequence is no longer applied. To describe the reality one should take in account that some metastable precipitates coexist [8].

α_{ssss} -> clusters -> GP, β", β', B', U1, U2, … -> β

3.4.2. The precipitates

3.4.2.1. Structure of the solid solution and early stages

Supersaturated solid solution is obtained just after quenching. Through this rapid cool down, the alloy's state is frozen almost in the same situation as it was before quenching. Thus if quenching was led out just after a long solution heat treatment, the SSSS has a large number of excess quenched in vacancies, which concentration is closed to concentration of vacancies before quenching and a random solute atoms distribution inside the aluminium matrix.

This situation is quite unstable. It trends to evolve toward an energetically lower state. Diffusion of the atoms, which is enhanced by the excess vacancies concentration leads to the formation of some clusters, so called embryo clusters [18]. Some Mg-clusters and Si-clusters were observed but also Mg-Si co-clusters. Some Si-rich clusters were observed in alloys with a large excess of silicon [21]

As a mechanism for the formation of these embryo clusters, it is widely thought that Silicon atoms diffuse and forms some first clusters which will attract afterwards the Mg atoms. [8]

3.4.2.2. GP-Zones

GP-Zones have been found to be fully coherent precipitates. Commonly they are seen as a bigger version of the Mg-Si co-clusters. They are very small, up to a few nanometres large, which make their direct observation very difficult [18]. Using HRTEM, it was recently possible to observe the GP-Zones directly [21]

From different observations, several models have been built for GP-Zones. Thomas' model was made to explain observation done in Al-Mg-Si alloys. In this description the GP Zones are an alternating of two rows Mg separated by one row Si. This gives an orthorhombic FCC based super cell. [7] Another model is Matsuda's model, which consists in an ordered arrangement of Mg and Si atoms with n layers pure Al in-between (where $n \geq 0$). Depending on n the arrangement is called $L1_n$. $L1_0$ and $L1_2$ are famous arrangements [7].

On figure 8, Thomas' model, $L1_0$, $L1_1$ and $L1_3$ arrangements of Matsuda's model are presented.. The red spheres are silicon, the black ones magnesium and the white ones aluminium.

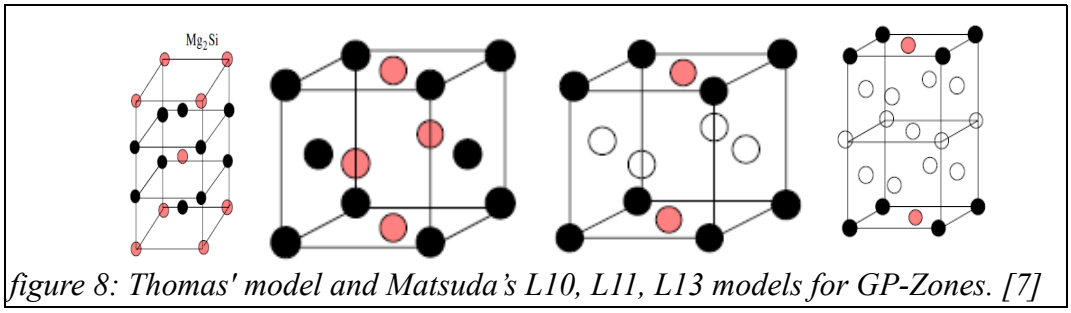

figure 8: Thomas' model and Matsuda's L10, L11, L13 models for GP-Zones. [7]

The question remains, whether GP-Zones are nucleation sites for β" precipitates. According to some experimental observations especially DSC scan, it is admitted that GP-Zones reverse before β" precipitates [18]. At higher temperatures it is assumed that GP-Zones do not reverse but evolve continuously toward β" precipitates and form so-called pre-β" precipitates with a structure, and a composition ($Mg_xAl_{5-x}Si_6$; with $0 \leq x \leq 5$) closed to β" and a smaller size. [18]

Structure of the GP-Zones depends on the alloy's composition. However the $MgSiAl_{10}$ and $(MgSi)_2Al_{10}$ are the most probable and thermodynamically favoured phases. [22]

3.4.2.3. β" precipitate

β" is technically the most important precipitate in the scope of precipitation hardening because this precipitate is responsible for peak hardness. [23].

The β" precipitates are generally observed as needle-shaped precipitate aligned along the <100> axis of the aluminium matrix. [18]. The length of the needles may reach 20 to 100 nm and the cross section is several nanometres large. β" precipitates are fully coherent along the b axis. It is a semi-coherent precipitate.

The structure of β" was found to be monoclinic with $C2_m$ group symmetry. Lattice parameters are a=15.16 Å, b=4.05 Å, c=6.74 Å, with angle β=105.3°. Composition is Mg_5Si_6. [8, 20]

Other lattice parameters were reported like a=15.3Å, b=4.05Å and c=6.83Å with angle β=105.5° for the same based centred monoclinic structure [24]

It was recently found, that a little change in the composition of the alloy could affect the structure of the β" precipitate. Excess of silicon is especially a decisive parameter for this influence [21]. However this was not widely reported.

It was found that the precipitate β" coexists with some other precipitate, especially the B' precipitate. Nevertheless β" is still considered as the precursor of the β' phase. [21]

3.4.2.4. β', B', U1 and U2 and C precipitates: the over-aged stages

Over-aged stages are all the precipitation stages appearing after the peak of hardness. As peak hardness is relied on the β" phase, the overaged phases consist of all phases that can be observed after β" phase. This includes several phases which will be presented in more detail.

Depending on the composition of alloy, and especially on excess of silicon, several metastable precipitates have been observed as precursor of the stable phase. The first metastable direct precursor of the stable phase was observed in the balanced alloys and was called the β' phases. However for excess Si alloys, some other phases have been observed. They have fully different properties, especially regarding density or geometry. Several designations might be found in literature for these phases. Usually, they are named, type A (or U1), type B (or U2) and type C. Later a B' phase was also observed.

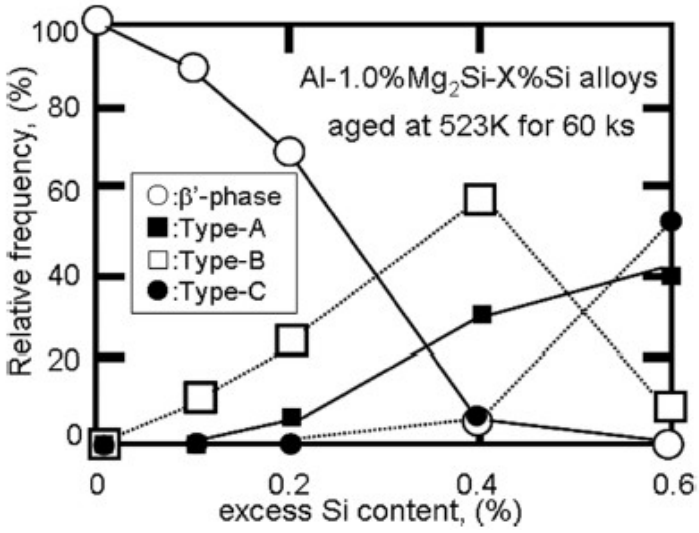

figure 9: relative frequency of precipitates in alloys with 1,0wt% Mg2Si aged at 250°C for 1000 min. [21]

β’ phase was found to be rod-shaped with a hexagonal structure with lattice parameters a=7.05 Å and c=4.05 Å [24, 25]. Some authors report other lattice parameters. For instance Marioara [8] reported $P6_3$ structure with the lattice parameters a=7.15 Å and c=4.05 Å. Each cell would have 6 Mg atoms and 3.33 Si atoms due to vacant sites. Figure 10 is a schematic presentation of the unit cell, show in part of the silicon atoms and the vacant sites in the lattice.

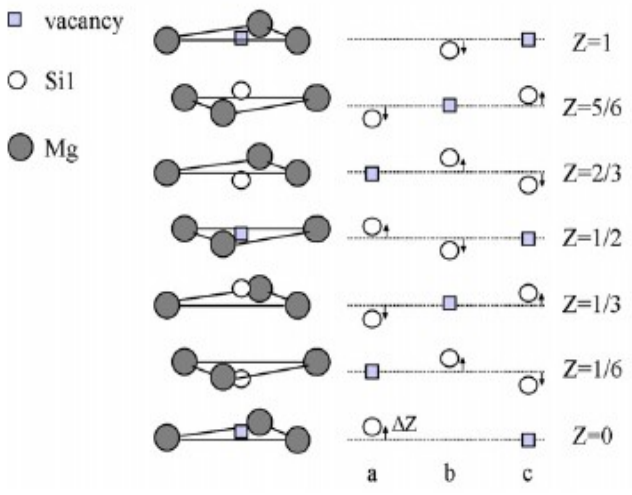

figure 10: schematic structure of β' phase : Si1 atoms, Mg atoms and vacant sites [20]

U1 precipitate is also sometimes called type A-precipitate. It is supposed to have a $MgAl_2Si_2$ composition, a hexagonal structure and P_{-3m1} group symmetry with the following lattice parameters: a=b=4.05 Å, c=6.74 Å, β=120°. They are commonly observed as needles of several hundreds nanometres length and about 15 nm diameter. [8, 20]

U2 precipitate is sometimes called type B precipitate. It is observed as needles. Structure was found to be P_{nma}. Composition MgAlSi and the lattice parameters a=6.75Å b=4.05Å and c=7.94Å [8]. It has 12 atoms per unit cell.

A C precipitate was also observed as ribbons up to 1μm long in some alloys. It has a Si:Mg ratio upper than 1, but the exact composition is still being inquired. It has a hexagonal structure with lattice parameters a=10.3Å and c=4.05Å.

The B' precipitate has a structure close to that of Q phase, but has been observed also in copper free alloys, like AA6061 [24] and has been observed as a lath-shaped precipitate [7]. It is assumed to have a Mg:Si atomic ratio close to 1 [8] and widely accepted to have the same composition as Q-precipitate, without copper with the formula $Al_4Mg_8Si_7$ [7]. The structure is hexagonal with lattice parameters a=10.4Å and c=4.05Å [8].

In a recent wok, relying on first-principles calculations, the Dutch physician van Huis could postulate a metastable energetically favourable phase, that was not observed so far and is called U3 [22]

3.4.2.5. Stable phases ß and Si

Stable phase which are observed in 6xxx-alloys is the stoichiometric precipitate Mg_2Si, called β precipitate. It is observed as incoherent platelets or cubes with a cross section which can be up to 20 µm [20]. It is not believed to contribute to strengthening [25]

Structure of this precipitate has been clarified a long time ago. It is known to have an anti-fluorite face centred cubic structure with lattice parameter a=6.39 Å. The group symmetry is $F_{m\text{-}3m}$ [26]

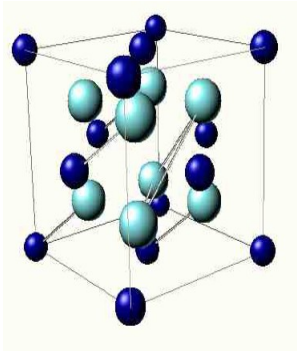

figure 11: the anti-fluorite structure of β precipitates [8]

Other stable phase which can appear in Al-Mg-Si alloys with excess of silicon is the diamond like silicon (group symmetry Fd3m´), with a lattice parameter of 5.43 Å. This phase has already been described in 3.2.

3.4.3. Effect of copper-addition

3.4.3.1. Influence on precipitation sequence

In many industrial alloys type 6xxx series, there are some other alloying elements. Very often, there is some manganese or some iron. These elements are rather impurities and they have no influence on the precipitation sequence.

However, in some alloys, copper is added. For instance 6111 alloys have about 0.7 wt. % copper in the composition. The reason for this copper adding is the enhancement of the precipitation kinetics and better hardening and physical properties [4, 8].

The quaternary system Al-Mg-Si-Cu is very complex and many equilibrium phases can be found. An overview is given in reference [15] in which this system is fully described. Figure 12 shows all possibilities for occurrence of stable phases.

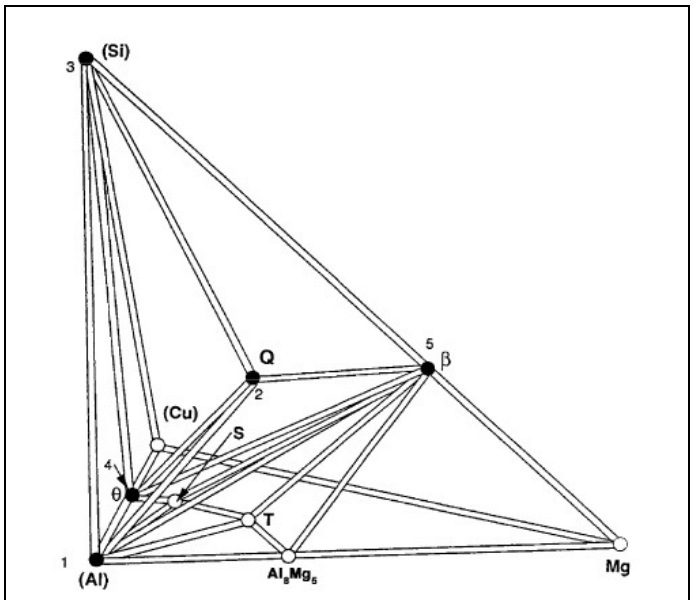

figure 12: stable phases in Al-Mg-Si-Cu alloys [15]

Presence of copper in 6xxx series does not affect significantly the precipitation sequence. Another stable phase is promoted, the quaternary Q-phase which can be observed along with the β stable phase [17].

This stable phase is also known for having some metastable precipitates like the Q' phase which has been observed along with the β' phases [17]. There might be some other metastable precursor to the Q phase, which is reported in some papers [15]. The metastable precursors, their structures and their numbers are still controversial.

3.4.3.2. Q' phase and other metastable precursors of Q-phase.

Q' was observed as a lath-like precipitate [8]. It seems that the only difference between the Q' and the Q precipitates is a matter of sizes. Some other metastable precursors have been observed too, like the QP and QC precipitates [15].

3.4.3.3 Q-phase

Q-phase is admitted to have a hexagonal with a=10.4 Å and c=4.05Å and has 21 atoms in a unit cell. The composition could be $Al_4Cu_2Mg_8Si_7$ [26, 24]. It is commonly observed as a lath-like precipitate. [19].

The exact composition of the Q precipitate is still controversial and several possible compositions have been proposed so far. [17]. However, the composition stated previously is the one which is currently accepted.

3.5. Testing methods

3.5.1. Difference Scaning Calorimetry (DSC)

Difference Scaning Calorimetry is a thermal analysis method which consists in measuring the heat flow difference between two samples, a reference sample and an inquired sample. Several device constructions are possible [33]. The so-called heat flow method was the only one that was used in this study. It is presented below, on figure 13.

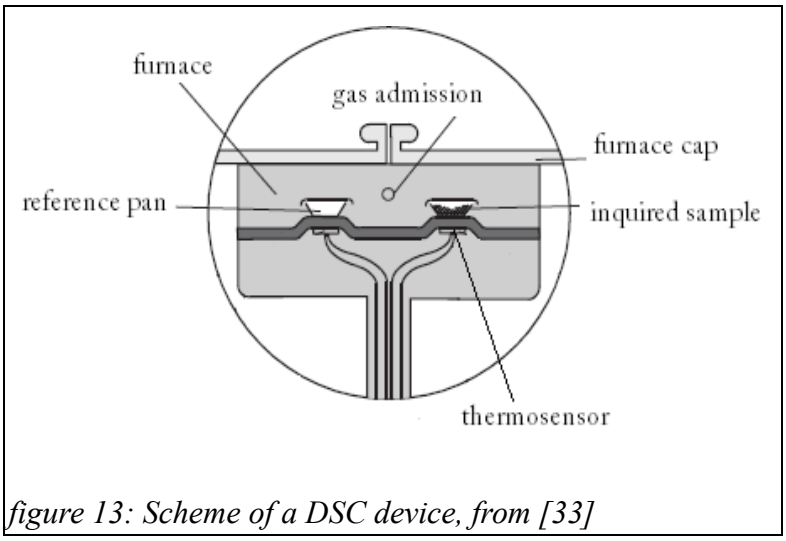

figure 13: Scheme of a DSC device, from [33]

In this construction, both samples are placed inside a single oven which is heated. Temperature difference between both samples is measured. In case of perfect symmetry of the physical properties no temperature difference will be measured. But if a difference appears, there will be a measurement, which is related to heat flow difference between both samples.

Heat flow difference can have several origins and can be due to microscopic phenomena, like, for instance precipitate formation or dissolution in metals alloys, phase transition, local melting. Precipitation processes release heat and induce exothermic peak that can be observed by DSC [25]

Heating rate used for DSC experiments has an influence on the shape of the curve observed. A slow heating rate shifts peaks to lower temperature in the DSC curve [25]. Moreover, a higher heating rate allows observing smaller effects, but will decrease the resolution. Other influencing parameters are the mass of the sample, and its geometry.

3.5.2. Dilatometer (TMA)

With increasing temperature and changes at the microscopic scale, the volume of a material can change. This change is partially due to expansion of material because of temperature increase and partially due to effective changes in volume induced through phase transformation, phase precipitation or precipitation dissolution. Through analysis of these volume changes, important information about the micro-structural

evolution of the material can be obtained. In TMA method a very small force typically about 0,001 (to 1N) will be inserted on sample to keep it in place. Length change will be measured by very sensible length transducer (sensibility: 100 nm) and will be recorded with time and temperature.

By using a dilatometer, it is possible to get information on the length change of one sample as a function of temperature. The coefficient of thermal expansion (CTE) is as in formula (3) [33].

$$\alpha = \frac{1}{l_0}\frac{\partial l}{\partial T} \tag{3}$$

In formula (3), original length of sample or reference length is l_0 , l is current length and T is current temperature. It is also possible to define a cubic coefficient of thermal expansion: [33]

$$\beta = \frac{1}{V_0}\frac{\partial V}{\partial T} \tag{4}$$

Here, V is the sample's volume and V_0 the reference volume of the sample. However for isotropic samples, these two values are linearly proportional to each other.

$$3 \cdot \alpha = \beta \tag{5}$$

Dilatometer measures the variation of length of a sample with regard to the reference length which is measured before starting the experiment. Length measurement must be very accurate in order to ensure a reliable value of coefficient of thermal expansion. The measurement relies often on inductive transducer, which allows to detect even small displacement and length changes. [33]

In aluminium alloys, CTE is in the order of 20 to 40 ppm/K

3.5.3. Other methods

During precipitation process, some properties of the alloy may be changed, as for instance resistivity. Because precipitates have different structures and properties than the matrix, resistivity of the sample changes with precipitation. . This method has been used with success in the past years [26, 25].

3.6. A short introduction to the MatCalc software.

3.6.1. The MatCalc software

The MatCalc software is a computation software which is being developed since the early 90s. It allows the simulation of thermo-kinetic process in materials, and the computation of equilibrium properties and precipitation kinetics.

The MatCalc software is based on Calphad approach and uses three different databases which deliver descriptions for thermodynamic properties, mobility and physical data. From these databases it is possible to compute phase diagrams and precipitation kinetics.

Precipitation kinetics is simulated by using classical nucleation theory. It is possible to simulate the evolution of precipitates' distribution, size, composition and further descriptive parameters. MatCalc allows also calculation of heat flow and volume. These calculations are especially important for comparison of simulated DSC and dilatometry results with experiments.

Models and the detailed thermodynamic approach of MatCalc is out of the scope of this study and will not present here. For more information, one can refer to related literatures such as [31].

3.6.2. MatCalc physical database

MatCalc physical database is a summary and a collection of values in order to perform computation of macroscopic properties such as volume. It contains density data, and the influence of the system composition on density.

The densities are presented as two lists of values: Reference value which corresponds to density of the phase at standard room temperature of T_0 = 298 K and their temperature dependency with respect to reference temperature. $\rho(T)-\rho(T_0)$

For phases which composition is changing like matrix, two models are available to describe the composition dependence of the density: Vegard's law or a model that consider the interaction parameters too. Vegard's law is described in a later part of this report.

4. Experimental

4.1. Materials and composition

In this work four materials are used. The composition is give in table [3]

Table 3: Composition of the alloys used during this work

Alloy	Si	Mg	Fe	Mn	Cu	Other
Al Si1.1	1.1 wt.%	≈0	≈0	≈0	≈0	≈0
Al-Cu 4,3	≈0	≈0	≈0	≈0	4.3 wt.%	≈0
AA6016	1.10 wt.%	0.35 wt.%	0.16 wt.%	0.07 wt.%	0.08 wt.%	0.02 wt.%
AA6082	0.9 wt.%	0.76 wt.%	0.41 wt.%	0.51 wt.%	0.09 wt.%	≈0

AA6016 and AA6082 materials were available as cold rolled sheets, with thickness of 1 mm and 1.5 mm respectively. These commercial alloys contain not only aluminium, magnesium, and silicon but also some other alloying elements in very small amounts.

The Al-Cu samples used were extruded laboratory made pure Al-Cu samples.

4.2. Preparation and heat treatment of the sample

DSC samples were punched in 6mm diameter from the materials. If necessary, thicknesses were reduced by grinding to reducing the weight and make them equal to the weight of a reference sample of pure aluminium (about 80 mg mass).

Dilatometer samples had been cut as small rod with 7mm (for Al-Cu sample) or 10mm (for all other samples) height. The cross-section of the rod depends on the material used and is not influencing the results.

Laboratory made Al-Cu 4.3 samples were homogenized before use. Homogenization carried out by isothermal heating at 480°C for 24 hours under normal air atmosphere. Metallographic analysis was carried out to make sure about the homogeneity of the sample

All samples were solution treated at 540°C to 560°C for at least 40 minutes and quenched in cold water. This state is called T4_fresh. Further heat treatments were carried out using DSC or dilatometer devices. Neither room temperature not artificial ageing has been carried out during this work.

4.3. Difference Scaning Calorimetry

For thermal analysis, DSC device type DSC2920 from the company TA Instruments was used.

DSC experiments were carried out with a constant heating rate of 5K/min in a temperature range from 30°C to 560°C.. A typical heat cycle is presented on figure 14. The reference sample used is a 6 mm circular disk of 99.99 % pure aluminium. For protection nitrogen with a flow of 50ml/min was used. The data collected by the device was processed by using the Origin Software of the company Origin-lab. Some experiments were carried out with a higher heating rate of 10K/min for AA6016 samples.

Nota Bene: On presenting the results of experiments, always exothermic reactions are shown as down peaks

4.4. Dilatometer

Another thermal analysis method used was dilatometer. Dilatometer tests were led out using 5K/min heating rate from 30°C to 560°C. The heat cycle is presented on figure 14. Like for DSC analysis, some AA6016 samples were tested with higher heating rate of 10K/min.

Cooling down of the sample occurred under nitrogen atmosphere with a flow rate of 100 ml/min. The vertical holding force used during this experiment was 0.05 N. The used device was the TMA 2940 Thermo-mechanical analyser from the TA Instruments company.

Data collected by the device was processed using the origin software of Origin-lab Company. The processing consisted of an interpolation with 300 to 450 points of the dilatation data followed by smoothing using symmetrical averaging smoothing of 5 points, a second interpolation with 60 to 80 points and finally numerical derivate with respect to temperature. This method aims to reduce the influence of noise in the data collection.

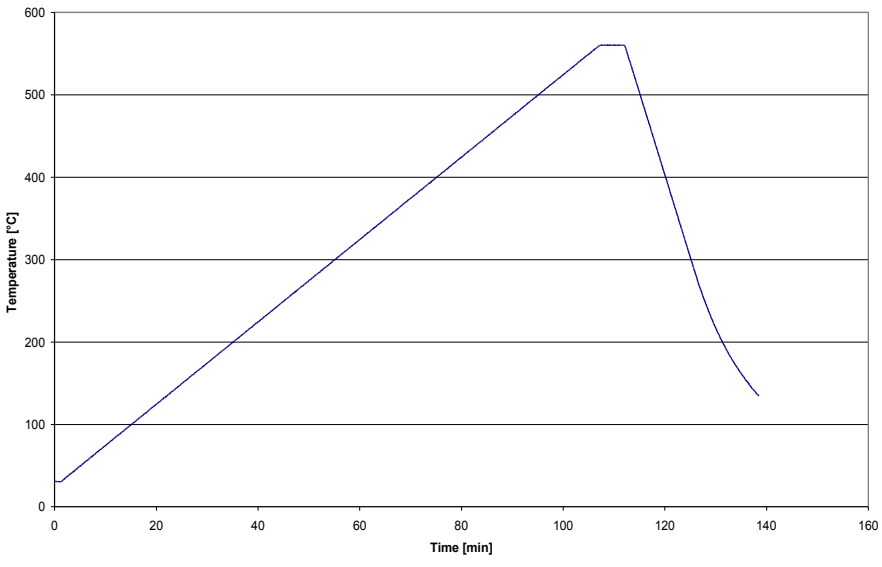

figure 14: Heat Cycle used for DSC and TMA experiments.

5. Simulation

5.1. Simulation using MatCalc

MatCalc simulation requires a script which describes the systems and the heat treatment. These scripts were developed by Mr. Peter Lang in the scope of his Ph.D. thesis. [32]. His work consisted especially in modelling the behaviour of AA6016 alloys. He adapted the input data for simulation of DSC experiments which results are described in part 6 of this study. The model parameters to adjust, is the interfacial energy, misfit of the single phases and nucleation sites. The aim is not tp present exhaustively each one of these parameters and the methodology of adaptation, as it is out of the scope of this study.

Using these scripts, Simulation of nucleation process and growth of precipitate could be carried out. After the computation of precipitation kinetics is achieved with MatCalc, the physical database can be loaded. MatCalc computes automatically the volume of one mole V_m of the system as a function of time and temperature. It is possible hence to plot the coefficient of thermal expansion (CTE) according to the following definition, which is deducted from equation (4):

$$CTE = \frac{1}{V_{m,ref}} \frac{\partial V_m}{\partial T} \tag{6}$$

In formula (6), $V_{m,ref}$ denotes the reference molar volume. This formula gives a CTE in K^{-1}. Units are commonly adapted for readability reasons and easy comparison with experimental values : equation (6) multiplied it by 100 (respectively by 10^6) leads to a result in %/K (respectively in ppm/K).

In order to be consistent with experiments reference volume is the volume of the system before starting heating up. It means the molar volume at 25°C. Once the CTE is plotted it can be compared to experiments or to other computational models.

In order to understand what is happening at the microscopic scale, Information on the phase fractions, size of precipitates (mean value, extreme values, …), and composition of non stoichiometric phases such as matrix or GP-Zones can be obtained with MatCalc.

For modelling the volume changes during heat treatment, several MatCalc versions (v 5.32, 5.4.0.019 and v 5.40.1.000) were used, according to the progress in programming and the software updates, were used. The thermodynamic database and the mobility database used were versions v0.10 (updated on February, 26th, 2010) and version 1.03 respectively.

The youngest computations were not carried out again with newest versions if the results were satisfying. The motivation for avoiding a new computation was time sparing and inquiry of more interesting systems.

5.1.1. Simulation of Al-Si system

For modelling of volume changes in the Al-Si systems, MatCalc version 5.32 was used with thermodynamics database version 1.010, mobility database version 1.03 and physical database with updated values for precipitates densities was used (v1.07).

5.1.2. Simulation of AA6016 alloy (Al-Mg-Si system)

Adjusting input parameters and calibrating the model for Al-Mg-Si system has been carried out by comparing the DSC simulation and experimental results. [32]. The approach is progressive and with changing kinetic input parameter on a physical interpretation base in order to match the DSC experiments with as less deviation as possible with simulation. The DSC simulation that have been used for this work were led out in the scope of another project at the Institute.

In the scope of modelling the volume changes in the Al-Mg-Si systems, MatCalc version 5.40.0.019 and 5.40.1.000 with thermodynamics database version 1.010, mobility database version 1.03 and physical database version 1.009 with updated values of the precipitates densities were used. Simulation of this system is still being improved. The presented results are that of 30st of September 2010.

5.1.3. Simulation for the Al-Cu system

The modelling of volume changes with MatCalc was started but the adjustment of thermokinetics input parameters within the existing time span of this work was not possible. This remains an open challenge of future works. However, first results are presented here.

5.2. Matcalc physical database

5.2.1. Precipitates density data

In order to carry out computation using MatCalc for simulation of the instantaneous CTE, the density of each phase that can appear in the system was computed. Using the data which are available in literature for the structure and lattice parameters, volume of the unit cell can be computed. Using the composition of the precipitate and the atomic mass, the weight of one unit cell is obtained. This requires however knowing the whole description of the precipitate and not just a stoichiometric formula of it, because some lattice sites may remain vacant, as it is for instance in the β'.

Using the weight of one unit cell and its volume, it is possible and easy to compute the density of each precipitate. For extending the physical database, densities of the required new phases have been calculated. The densities obtained have been multiple checked by computing volumetric misfit of the precipitates with respect to aluminium and comparing the results with available values in literature.

Volumetric misfit is defined as the difference between atomic volume of the phase and the atomic volume of aluminium divided by the atomic volume of aluminium

$$\delta = \frac{V_{at} - V_{at,ref}}{V_{at,ref}} = \frac{V_{at}}{V_{at,ref}} - 1 \qquad (7)$$

In table 4, the most probable or commonly admitted structure, lattice parameter, composition and number of atoms per unit cell for each precipitate are given.

In order to save place some abbreviations have been used as follows:"geo(metry)", C means cubic, M means monoclinic, H means hexagonal, O orthorhombic and T means tetragonal.

Table 4: Composition, geometry and lattice parameters of different precipitates

				Lattice parameters				
precipitate	Compos	At cell	geo	a [Å]	b [Å]	c [Å]	β	Ref
Pure Al	Al	4	C	4,04	/	/	/	[1]
GP-Zones $L1_0$	MgSi	4	C	4,05	/	/	/	[7]
β"	Mg_5Si_6	22	M	15,16	4,05	6,74	105,3°	[20]
β'	Mg_9Si_5	14	H	7,15	/	4,05	/	[8]
U1	$MgAl_2Si_2$	5	H	4,05	/	6,74	/	[20]
U2	MgAlSi	12	T	6,75	4,05	7,94	/	[8]
B'	$Al_4Mg_8Si_7$	19	H	10,4	/	4,05	/	[8]
β	Mg_2Si	12	C	6,39	/	/	/	[26]
Silicon	Si	8	C	5,43	/	/	/	[6]
Q	$Al_4Cu_2Mg_8Si_7$	21	H	10,4	/	4,05	/	[26]
θ"	Al_3Cu	8	T	4,05	4,05	7,68	/	[11]
θ'	Al_2Cu	6	T	4,05	4,05	5,81	/	[11]
θ	Al_2Cu	12	T	6,05	6,05	4,87	/	[11]
S	$CuMgAl_2$	16	O	4,00	9,23	7,14	/	[16]
S'	$CuMgAl_2$	16	O	4,04	9,25	7,18	/	[16]

Table 5 shows summary of all important parameters needed for physical database and the obtained misfit to compare with literature. Given values: density, volumetric misfit (vol. misfit) and molar mass of the precipitate, were computed directly from the data in table 4.

As MatCalc physical database gives the possibility to compute temperature dependant values for densities, it was assumed, that the temperature dependence is the same for all precipitates and to be close to the β" precipitates. The reason for this is the lack of information about the temperature dependence of the metastable precipitates. Moreover as it will be shown later the contribution to CTE given by the temperature dependence of the density is negligible in compare to the contribution of matrix or precipitate formation. So, to be coherent with methodology all precipitates' densities has been changed considering temperature effect.

Temperature dependence of density for β" precipitate was computed and given to us by Mr. Erwin Powoden-Karadeniz, Ph.D. Methodology used for this computation is out of the scope of this study.

Table 5: Atomic volume, molar lass, density and volume misfit of the precipitates

precipitate	Atomic volume [m^3]	Molar mass	**Density [kg/m^3]**	Vol. misfit
Pure Al	$1.648\ 10^{-29}$	26.98 g/mol	**2 718,6**	Ref. lattice
GP-Zones L10	$1.661\ 10^{-29}$	26.20 g/mol	**2 619,3**	0,79 %
β"	$1.8143\ 10^{-29}$	26,37 g/mol	**2 413,9**	10,07 %
β'	$1,9211\ 10^{-29}$	25,66 g/mol	**2 218,1**	16,57 %
U1	$1,9148\ 10^{-29}$	26,89 g/mol	**2 331,7**	16,20 %
U2	$1,8088\ 10^{-29}$	26,46 g/mol	**2 428,9**	9,76 %
B'	$1,9966\ 10^{-29}$	26,26 g/mol	**2 183,6**	21,17 %
β	$2,174\ 10^{-29}$	25,57 g/mol	**1 953,1**	31,92 %
Silicon	$2,001\ 10^{-29}$	28,09 g/mol	**2 331,1**	21,42 %
Q	$1,8065\ 10^{-29}$	29,81 g/mol	**2 739,4**	9,69 %
θ"	$1,5746\ 10^{-29}$	36,12 g/mol	**3 803,9**	-4,45 %
θ'	$1,5883\ 10^{-29}$	39,17 g/mol	**4 093,4**	-3,64 %
θ	$1,4855\ 10^{-29}$	39,17 g/mol	**4 377,2**	-9,86 %
S	$1,6476\ 10^{-29}$	35,46 g/mol	**3 573,5**	≈0
S'	$1,6770\ 10^{-29}$	35,46 g/mol	**3 510,8**	1,82 %

Within the scope of this study, the temperature dependence of virtual FCC silicon and virtual FCC magnesium were computed. In order to do it, data from literature (molar volume) and Calphad methodology [34] was used.

For FCC Magnesium, literature gives the following molar volume polynomial as a function of temperature.

$Vm = 13{,}40454 + 8{,}357\cdot10^{-4}T + 4{,}40\cdot10^{-7}T^2 + 2{,}14/T.$

Using the molar mass of magnesium, one can obtain the density at 298K: $\rho = 1774{,}83$.

The same with Silicon in FCC structure can be achieved. The following molar volume was found in literature [34].

$Vm = 9.13309 + 1.485\cdot10^{-4}T + 7.0\cdot10^{-7}T^2 + 7.84/T - 380/T^2$

The following value is obtained: T=298K, $\rho = 3060{,}10$

5.2.2. Composition dependence of the matrix

A further important advantage with MatCalc is to set up the composition dependence of non stoichiometric phase. In the scope of this study was considered. The problem of estimating the density of matrix with varied chemical composition as a function of time and temperature is not an easy task. Many models have been developed. The most popular one is Vegard's law. Interaction parameters can also be used and can be computed through experiments. The popularity of these models relies

on their simplicity and good results. There exist more sophisticated methods relying on continuum mechanics computation but they lead to long and difficult computation although they bring more reliable outputs [35].

MatCalc uses a CALPHAD type approach and includes interaction parameters which are given in the physical database under the description such as PARAMETER DP(FCC_A1,AL,MG:VA:0) for the influence of Magnesium. Figure 15 is an extract which shows these parameters for Mg and Si and the syntax of the physical database.

```
$ Al-Mg-Si system: interactions, regarding to the new end members FCCMG and FCCSI,
PARAMETER DP(FCC_A1,AL,SI:VA;0) 2.98150E+02       -250;    6.00000E+03   N REF on !
PARAMETER DP(FCC_A1,AL,MG:VA;0) 2.98150E+02       -300;    6.00000E+03   N REF on !
```

As an example, in order to choose these parameters, work of Hallstedt [34] which reviewed literature and computed composition dependence of binary Al-Mg and Al-Si systems has been used. His results is shown on figures 16 and 17. To reproduce these curves with MatCalc by using the previously introduced parameters, the thermodynamic database is loaded and binaries system (Al-Si) and (Al-Mg) were set up. Through plotting the molar volume versus composition of the phase, one could adapt the results which afterwards can be added to the physical database. The obtained results have been presented on figure 15.

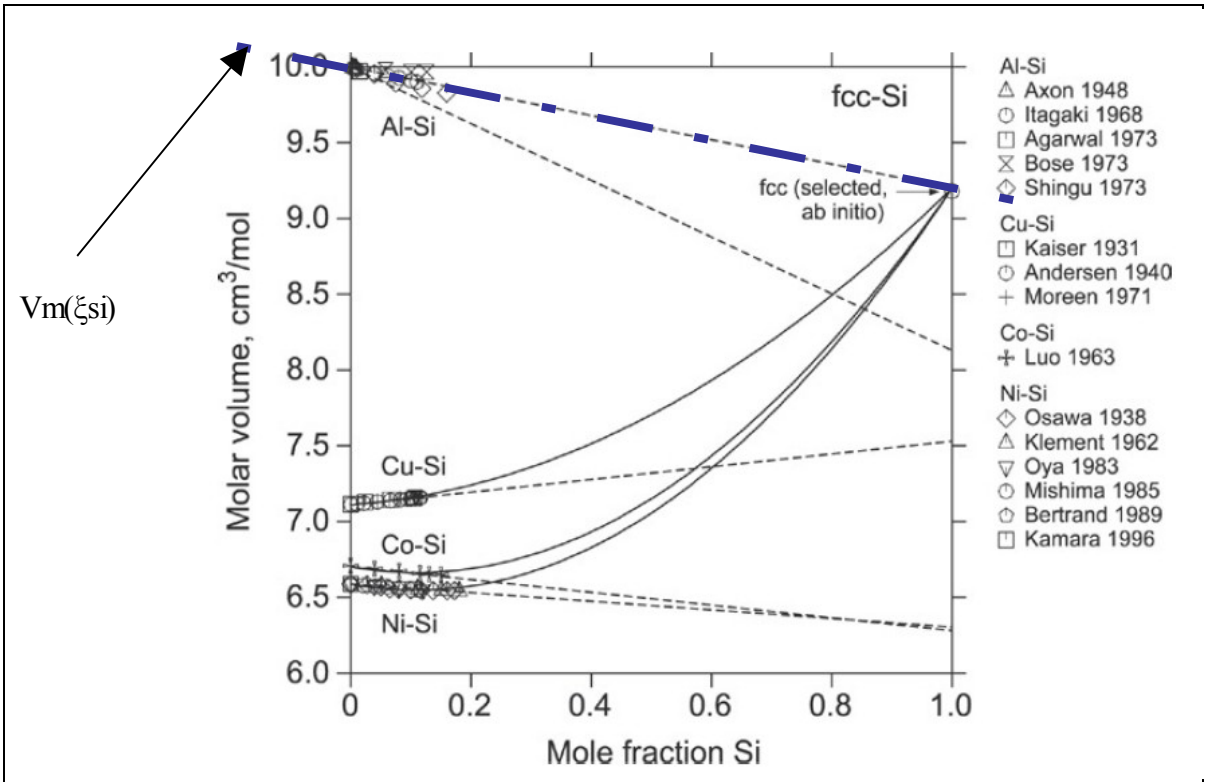

figure 16: Composition dependence of molar volume of several Si involving systems [34]

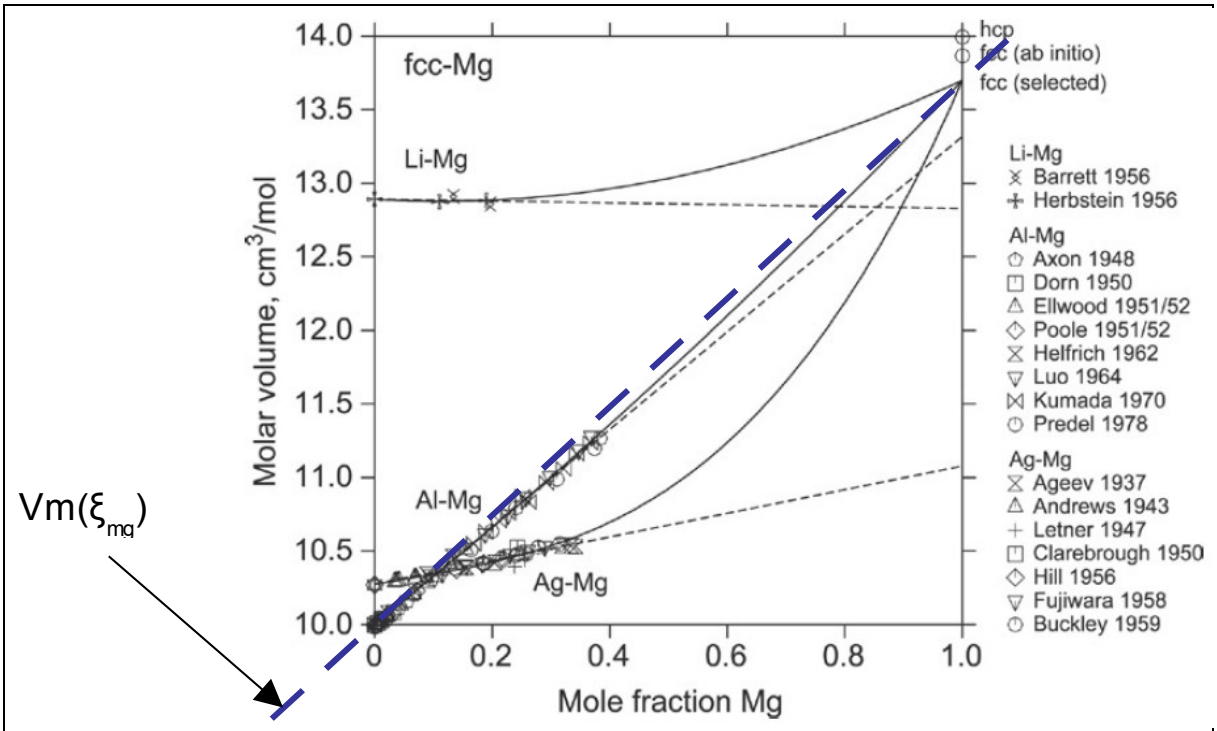

figure 17: Composition dependence of molar volume of several Mg involving systems [34]

5.3. Models for comparison

5.3.1. Starting point of modelling of volume changes

The problem of correlating the macroscopic volume changes to microscopic changes is not trivial. There are several effects which contribute to the volume changes, like formation and dissolution of precipitates, but also composition changes in the matrix.

For using the Software MatCalc including suitable thermodynamic and mobility database for thermo-kinetic simulation, an appropriate physical database to calculate the instantaneous coefficient of thermal expansion is required. However different approaches, partially independent to MatCalc approach, have been tried and the results were compared with MatCalc obtained results. The aim is to get a better understanding of the involved parameters. These models are presented in the present section 5.3

A dilatometer experiment allows us computing coefficient of thermal expansion (called α) usually expressed in ppm K^{-1} which is defined with formula (3). From formulas (4) and (5), for isotropic materials, the CTE can be linked to the volume changes.

$$\alpha = \frac{1}{3 \cdot V_0} \frac{dV}{dT} \tag{8}$$

V denotes here the volume of the sample and V_0 denotes the volume of the sample at a chosen reference state (for instance at 298K after quenching). In addition,

volume of a heterogeneous alloy can be computed easily. As volume is an extensive parameter, the volume of a given piece is the summation over all volume of each phase. The volume of the matrix phase will be denoted through V_m and the volume of each of the other n phases will be denoted V_i.

$$V = V_m + \sum_i V_i \tag{9}$$

Actually, using a thermodynamics computation program, like MatcCalc, it is possible to get phase fraction data. Using the density of the phase *i* as ρ_i and the density of the matrix as ρ_m), weight phase fraction φ_i can be related to the volume. Defining m_s as the total mass, equation (9) is transformed in the following:

$$V = m_s \cdot \left(\sum_i \frac{\phi_i}{\rho_i} + \frac{1 - \sum_i \phi_i}{\rho_m} \right) \tag{10}$$

Taking the derivative of above equation with respect to temperature, equation (11) is found:

$$\frac{dV}{dT} = m_s \cdot \left(\sum_i \left(\frac{1}{\rho_i} \frac{d\phi_i}{dT} - \frac{\phi_i}{\rho_i^2} \frac{d\rho_i}{dT} \right) - \frac{1}{\rho_m} \cdot \sum_i \left(\frac{d\phi_i}{dT} \right) - \frac{1 - \sum_i \phi_i}{\rho_m^2} \frac{d\rho_m}{dT} \right) \tag{11}$$

$$\frac{dV}{dT} = m_s \cdot \left(\sum_i \left(\left(\frac{1}{\rho_i} - \frac{1}{\rho_m} \right) \frac{d\phi_i}{dT} \right) - \sum_i \left(\frac{\phi_i}{\rho_i^2} \frac{d\rho_i}{dT} \right) - \frac{1 - \sum_i \phi_i}{\rho_m^2} \frac{d\rho_m}{dT} \right) \tag{12}$$

$$\alpha = \frac{m_s}{3 V_0} \cdot \left(\sum_i \left(\left(\frac{1}{\rho_i} - \frac{1}{\rho_m} \right) \frac{d\phi_i}{dT} \right) - \sum_i \left(\frac{\phi_i}{\rho_i^2} \frac{d\rho_i}{dT} \right) - \frac{1 - \sum_i \phi_i}{\rho_m^2} \frac{d\rho_m}{dT} \right) \tag{13}$$

From the software MatCalc, the weight fraction of each phase and its derivative with respect to temperature can be easily obtained. The remaining parameter to compute is the density as a function of temperature for each phase.

If it is assumed that all precipitates are stoichiometric, which implies that they have a fixed composition, their densities at a reference temperature can be calculated using crystallographic data from the literature. To compute the density of the matrix is not an easy task. The matrix has no fixed composition and not only temperature, but also the chemical evolution in the matrix due to precipitate and dissolution will affect its density.

Different methodology with deferent degree of simplification to compute the density and its derivative with respect to temperature has been used. The first idea is to assume that the density of the matrix is close to the density of aluminium. The second idea is to take in to account that the matrix contains not only aluminium but also other alloying elements.

5.3.2. Basic model (matrix density close to aluminium density)

Simplified model for the length variation of the sample would rely on the assumption that matrix density is very close or equal to aluminium matrix density. In this case, the formula (13) for CTE will reduce to the following formulas (14) and (15) (see table 6 for notation and units).

Table 6: Notation and units for part 5.3

variable	Description	unit	Taken from
α	Coefficient of thermal expansion	K^{-1}	
T	Temperature	K	
$\rho_{al,0}$	Reference density of aluminium	kg/m^3	From database
ρ_{al}	Density of aluminium	kg/m^3	From database
ρ_i	Density of phase i	kg/m^3	From database
φ_i	Weight fraction of phase i	1	From MatCalc

$$\alpha = \frac{m_s}{3 V_0} \cdot \left(\sum_i \left(\left(\frac{1}{\rho_i} - \frac{1}{\rho_{al}} \right) \frac{d \phi_i}{dT} \right) - \sum_i \left(\frac{\phi_i}{\rho_i^2} \frac{d \rho_i}{dT} \right) - \frac{1 - \sum_i \phi_i}{\rho_{al}^2} \frac{d \rho_{al}}{dT} \right) \tag{14}$$

$$\alpha = \frac{\rho_{al,0}}{3} \cdot \left(\sum_i \left(\left(\frac{1}{\rho_i} - \frac{1}{\rho_{al}} \right) \frac{d \phi_i}{dT} \right) - \sum_i \left(\frac{\phi_i}{\rho_i^2} \frac{d \rho_i}{dT} \right) - \frac{1 - \sum_i \phi_i}{\rho_{al}^2} \frac{d \rho_{al}}{dT} \right) \tag{15}$$

5.3.3. Density of the matrix using Vegard's law

5.3.3.1. Vegard's law

When a solid solution, composed of several kinds of atoms, is considered, one may wonder how the presence of atoms of different size will affect the density of the sample. The vegard's law is helpful to find a way to solve this problem [1].

Through the observation of the solid solution of two salts, Vegard developed a law correlating the different lattice parameters and an effective lattice parameter of the structure. The effective lattice parameters were found to vary almost linearly with the solute concentration, as a weighted mean of the lattice parameters of the solute and the solvent [36]

$$a_{eff} = \xi \cdot a_s + (1 - \xi) \cdot a_m \tag{16}$$

Where a_{eff} is the effective parameter of the solid solution, ξ is the molar fraction of alloying element, a_m is the atomic radius of the matrix element and a_s is the atomic radius of the alloying element.

It is assumed that this law can be generalised to a more complicated system with n alloying elements, extending the previous notation.

$$a_{eff} = \sum_i \xi_i \cdot a_i \tag{17}$$

ξ_i denotes here the molar fraction of each phase (matrix included) and a_i the lattice parameter of each phase.

Using formula (17) for aluminium alloys is not trivial. The common alloying elements do not have all FCC structures: Silicon is diamond-like, Magnesium and Zinc are hexagonal closed package structure. These elements do not exist as FCC structure at room temperature and normal pressure. However, a virtual lattice parameter of FCC structure that does not exist can be used for solute atoms. This will be described in the following paragraphs.

5.3.3.2. First approach: calculating temperature independent nonstable FCC lattice parameters for non FCC elements

With the assumption that in FCC lattice, the closest package is in diagonal and as the diagonal is hence equal to 4 atomic radii $r_{i,}$ virtual FCC lattice parameter can be calculated.

$$4 \cdot r_i = a_i \cdot \sqrt{2} \quad \Leftrightarrow \quad a_i = r_i \cdot 2\sqrt{2} \tag{18}$$

FCC lattice parameters calculated for Silicon, Zinc, and Magnesium are summarized in the following table.

Table 7: Atomic radii and lattice parameters of virtual FCC structures [1]

Element	Atomic radius	$a_{FCC,\text{ virtual}}$
Si	132 pm	373 pm
Mg	160 pm	453 pm
Zn	138 pm	390 pm
Al	143 pm	403 pm

There are different kinds of definitions for the atomic radius, which lead to slightly different results. Here atomic radius is considered as the mean distance of the nucleus of an atom to its surrounding cloud of electron in fundamental (i.e. non excited) state. This one was chosen.

5.3.3.3. Second approach: calculating nonstable FCC lattice parameter as a function of temperature based on experimental data

Another approach relies on experimental data, thermodynamics and CALPHAD approach. The molar volume of each element in each structure is described by a single polynomial expression as a function of temperature [34]. The method used is explained in details in the paper [34] but the detail of this computation is out of the scope of this study.

From the molar volume V_m and the Loschmidt-Avogadro number (which is the number of atoms in a mole, N_L=6,022 1023 mol-1), a virtual lattice parameter can be computed with formula (19)

$$V_m = \frac{N_L \cdot a^3}{4} \quad \Leftrightarrow \quad a = \left(\frac{4 \cdot V_m}{N_L} \right)^{1/3} \tag{19}$$

From literature [34], the temperature dependence of molar volume of FCC virtual structures for Mg and Si are given in table 8.:

Table 8: Molar volumes for FCC elements

Element	$V_m(T)$ [cm3/mol]
Magnesium	$13{,}40454 + 8{,}357 \cdot 10^{-4}\,T + 4{,}40 \cdot 10^{-7}\,T^2 + 2{,}14 / T$
Silicon	$9{,}13309 + 1{,}485 \cdot 10^{-4}\,T + 7{,}0 \cdot 10^{-9}\,T^2 + 7{,}84 /T - 380 /T^2$

5.3.3.4 Expression of density derivative, general case

Pure aluminium, as already mentioned in the introduction shows a FCC structure with a_{al}=404 µm lattice parameter at room temperature. The elementary cell of FCC structures has 4 atoms per cell. See formula number (19) to get lattice parameter from molar volume. Considering the presence of other alloying elements (with M_i as molar mass and ξ_i as molar fraction of the matrix) one can express the mean molar weight M as being:

$$M = \sum_i \xi_i M_i \tag{20}$$

Thus a composition depend expression for density of the matrix can be found:

$$\rho_m = \frac{4 \cdot \sum_i \xi_i M_i}{N_L \cdot \left(\sum_i \xi_i a_i \right)^3} \tag{21}$$

Both lattice parameters a_i and phase compositions ξ_i might be temperature dependant. Taking derivative of the above formula along T, the following expression (formula [22]) is found.

$$\frac{d\rho_m}{dT} = \sum_i \left(\frac{\partial \rho_m}{\partial \xi_i} \frac{d\xi_i}{dT} \right) + \sum_i \left(\frac{\partial \rho_m}{\partial a_i} \frac{da_i}{dV_{M,i}} \frac{dV_{m,i}}{dT} \right) \tag{22}$$

The derivatives involved in the above equation can be easily computed.

$$\frac{\partial \rho_m}{\partial \xi_i} = \frac{4}{N_L} \left(\frac{M_i \left(\sum_j \xi_j a_j \right) - 3\, a_i \left(\sum_j \xi_j M_j \right)}{\left(\sum_j \xi_j a_j \right)^4} \right) \tag{23}$$

$$\frac{\partial \rho}{\partial a_i} = \frac{-12 \cdot \xi_i}{N_L} \frac{\sum_j \xi_j M_j}{\left(\sum_j \xi_j a_j \right)^4} \tag{24}$$

$$\frac{da}{dV_m} = \frac{1}{3} \cdot \left(\frac{4}{N_L V_m^2} \right)^{1/3} \tag{25}$$

5.3.4. Summary

Both MatCalc and a numerical processing tool (for instance excel) will be used in order to get the curves of dilatometer simulation. From MatCalc, the molar phase fractions, the matrix composition (molar fraction of each alloying element into the matrix) and their temperature derivative are obtained. From physical database, the density data and its temperature derivative for each phase and lattice molar volumes of non existing FCC structures are found.

The formulas (15), (26) and (28) can be implemented in excel and thus several models for computing the volume change of matrix with different simplifications are used. As explained before, the comprehensive models is the general model implemented in MatCalc. Comparison of these different models with MatCalc just shows the effect of each parameter which is omitted due to simplifications assumed and involved.

- **Model A**: density of matrix is density of aluminium
- **Model B1**: using Vegard's law and fixed, non temperature dependent, FCC lattice parameters for virtual unstable Mg and Si.
- **Model B2**: using Vegard's law and temperature dependent, FCC lattice parameters for virtual unstable Mg and Si.
- **Model C:** MatCalc computation

For each model B1 and B2, the expression of the coefficient of thermal expansion is as the following:

$$\alpha = \frac{\rho_{m,0}}{3}\cdot\left(\sum_i\left(\left(\frac{1}{\rho_i}-\frac{1}{\rho_m}\right)\frac{d\phi_i}{dT}\right)-\sum_i\left(\frac{\phi_i}{\rho_i^2}\frac{d\rho_i}{dT}\right)-\frac{1-\sum_i\phi_i}{\rho_m^2}\sum_i\left(\frac{\partial\rho_m}{\partial\xi_i}\frac{d\xi_i}{dT}\right)\right)$$

$$\text{with}\quad \rho_m = \frac{4\sum_i \xi_i M_i}{N_L\left(\sum_i \xi_i a_i\right)^3} \qquad (26)$$

$$\text{and}\quad \frac{da_i}{dT}=0$$

For the so-called model B2, the CTE is given by the follwing formula (27)

$$\alpha = \frac{\rho_{m,0}}{3}\cdot\left(\sum_i\left(\left(\frac{1}{\rho_i}-\frac{1}{\rho_m}\right)\frac{d\phi_i}{dT}\right)-\sum_i\left(\frac{\phi_i}{\rho_i^2}\frac{d\rho_i}{dT}\right)-\frac{1-\sum_i\phi_i}{\rho_m^2}\sum_i\left(\frac{\partial\rho_m}{\partial\xi_i}\frac{d\xi_i}{dT}+\frac{\partial\rho_m}{\partial a_i}\frac{da_i}{dV_{m,i}}\frac{dV_{m,i}}{dT}\right)\right)$$

$$\text{with}\quad \rho_m = \frac{4\sum_i \xi_i M_i}{N_L\left(\sum_i \xi_i a_i\right)^3}$$

$$\text{and}\quad \frac{da_i}{dV_m}=\frac{1}{3}\left(\frac{4}{N_L V_m^2}\right)^{1/3}$$

5.3.5 Limitation and amelioration of Vegard's law

There exists some derivation of Vegard's law concerning the alloys [16, 23]. For a high amount of alloying element, the assumption that the effective lattice parameter is a linear combination of lattice parameter of elements in the same structure is no longer true. In order to be more accurate, the effect of strain stress created through the presence of elements of different sizes should be taken in to account [5, 6]. This brings a better approximation of the effective lattice parameter. This effect and temperature dependent effect is already included in semi empirical method used in reference [34].

5.4. A short summary on simulation

In order to simulate and compute numerically the coefficient of thermal expansion of a sample with a given composition, three different models were used.

Table 9: Summary of the models

Model	**Matrix composition dependence**	**Effect of vacancies**
Model A	no	Not considered
Model B1	Yes (Vegard's law),	Not considered
Model B2	Yes (modified Temp. dependent Vegard's law)	Not considered
Model C (MatCalc)	Yes (interaction parameter)	Considered

Calculation of thermal expansion with MatCalc includes the following effects:

- Formation and dissolution of precipitates
- Changes in matrix due to composition change during the process, interaction between alloy elements and expansion changes
- Expansion of all phases (changes in density)

MatCalc modelling is the most sophisticated.

6. Results

6.1. Pure Aluminium

6.1.1. Dilatometry

Results of dilatometry testing of a pure aluminium sample is given in figure 18, tested with a heating rate of 5 K/min. As is expected, the instantaneous expansion curve is close to a line and no significant dilatation or contraction peaks exist. This is considered as a reference curve and all further dilatometry experiments can be compared with this one.

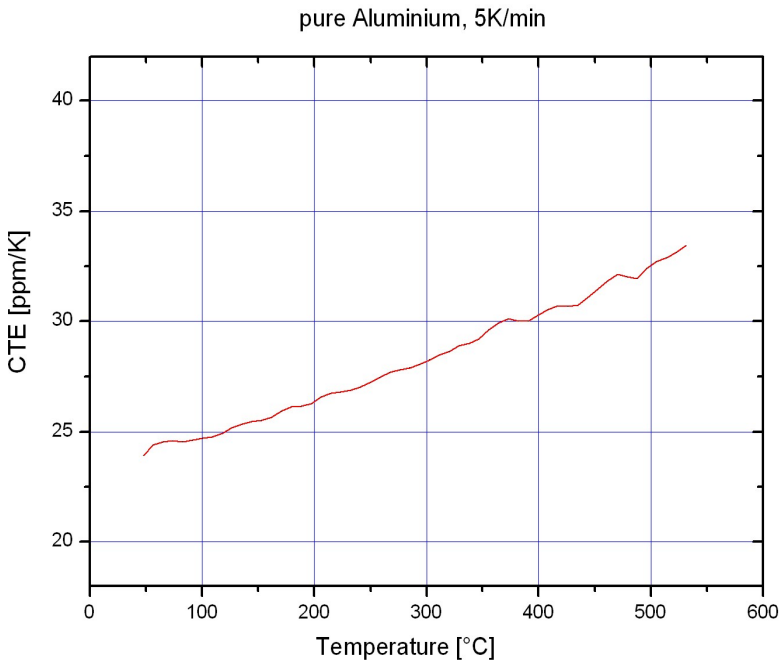

figure 18: Experimental results for CTE of pure Aluminium

6.1.2. MatCalc computation

In order to plot the CTE of pure aluminium with MatCalc, thermodynamic database must be loaded and elements aluminium, vacancy, and a third element, for instance Silicon must be selected. The phase FCC_A1 corresponding to the matrix must be selected. The composition of the matrix must be set with a value of silicon as close as possible to 0 wt.% and the computation can be started. Afterwards, physical database is loaded and a given temperature range in which the CTE must be computed is chosen.

As a result of MatCalc simulation, the molar volume of pure aluminium will be computed and plotted and MatCalc allows taking the derivative of the result and

dividing by 3 to convert to CTE. The result presented in figure 19 is obtained with MatCalc version 5.40.0.019, using physical database version 1.007 and thermodynamic database version 10. The temperature range was set between 20°C and 560°C.

The result is close to a line and no peak can be observed. Simulated values are in good agreement with the experimental results. Thus a good conformity between modelling and experiment can be observed for pure aluminium.

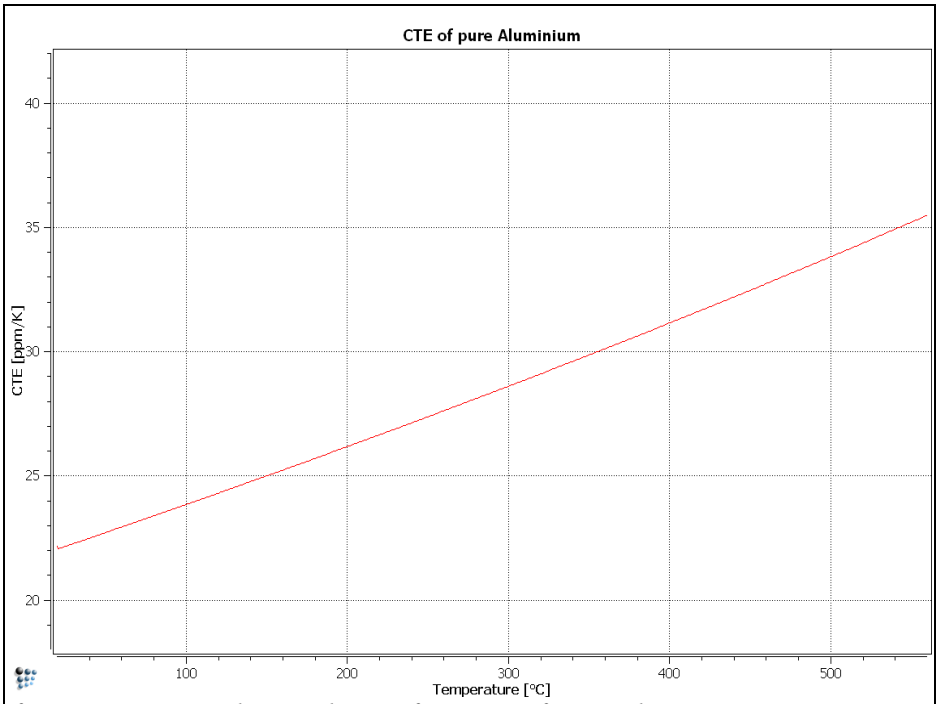

figure 19: MatCalc simulation for CTE of pure aluminium

6.2. Aluminium Silicon Alloys

6.2.1. Difference Scaning Calorimetry

The DSC Curve of Aluminium Silicon alloy (Al-Si 1.1) in the T4_fresh state is presented in figure 20. It contains one exothermic and one endothermic peak. For the presented experiment which was carried out with a heating rate of 5K/min, the first peak occurs at 250°C and is exothermic. The second one is endothermic and is about 450°C.

The reproducibility was ensured. Although as can be noticed, the heights of the peaks could hardly be reproduced, their positions are reproduced with a very good precision (see the two runs in Figure 20).

6.2.2. Dilatometry

In figure 21, CTE of Al-Si 1.1 in T4_fresh state is presented. This experiment was carried out with a heating rate of 5K/min. In temperature range from 200 to 300°C one large dilatation peak can be observed. It reaches a maximum of about 37 ppm/K at a temperature of 250°C. A second contraction peak, corresponding to Si dissolution can be observed between 300 to 500°C.

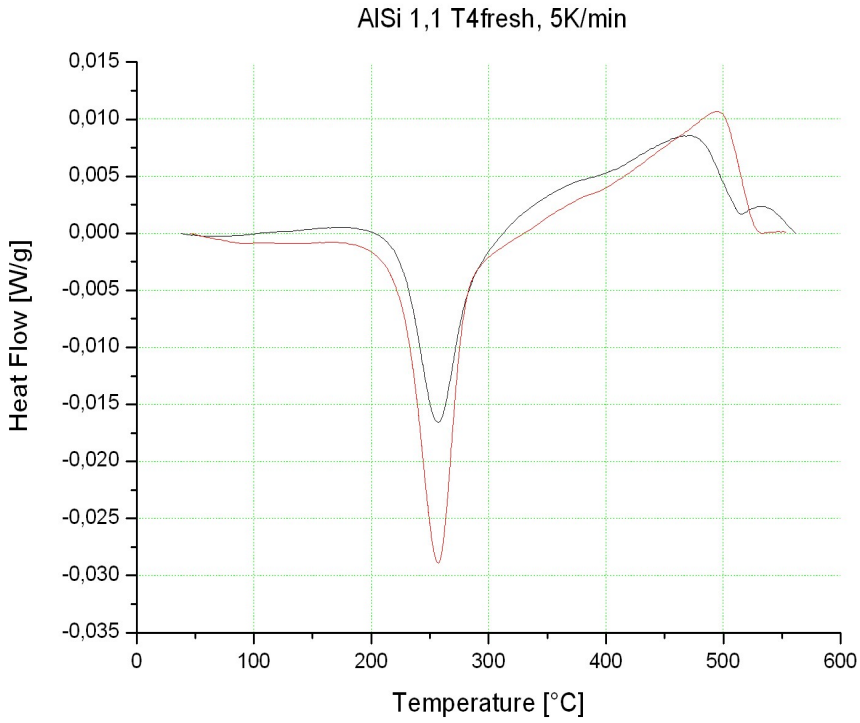

figure 20: DSC results Al-Si 1,1 wt.%, T4 fresh, 5K/min
Legend : run 1 is in blue and run 2 in red

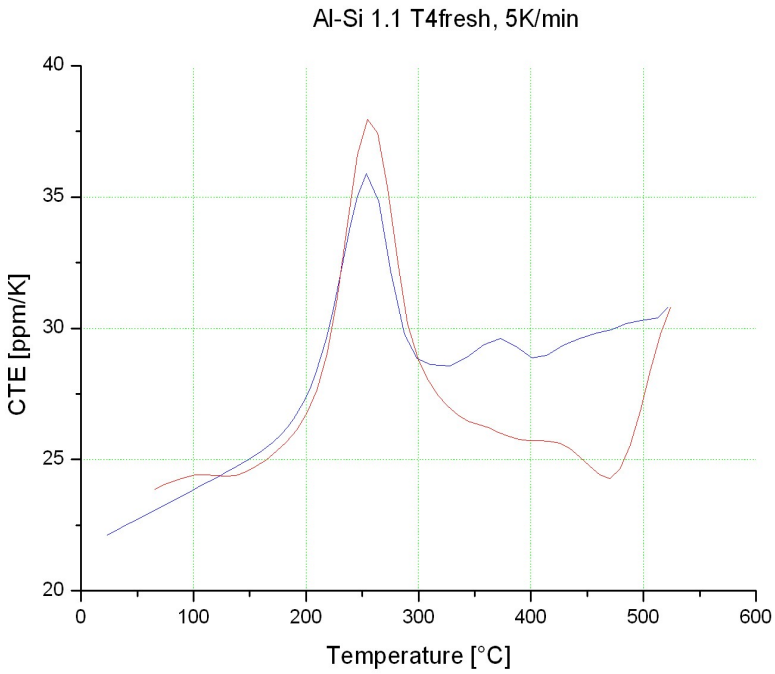

figure 21: TMA results for Al-Si 1,1 wt.% T4 fresh, 5K/min
legend : run 1 is in blue and run 2 in red

6.2.3. Results of MatCalc computations

Simulation was performed with version 5.32 of MatCalc. Thermodynamic database version 10, diffusion database version 3 and physical database 1.007 were used for the calculation. Elements Al, Si and Vacancies and phases FCC_A1 and SI_DIAMOND were selected. The amount of silicon was set to 1.1 wt.%.

The MatCalc computes the phase fractions. In this case, there are only two phases which can coexist, the FCC aluminium matrix which can also contain some solute silicon atoms and the silicon precipitate, which has a diamond structure. The phase fraction of the latter is presented of curve 22. On this figure, silicon precipitates are observed to start forming at about 180°C and the volume fraction is maxum at about 300°C. At higher temperature, silicon precipitates dissolve and thephase fracion is reduced progressively. At 520°C, no more precipitate is avalaiblen it remains the aluminium solid solution and the silicon atoms are randomly distributed in it.

From the phase fraction data, one can perform the simulation of CTE with the models A and B2 presented in part 5 or directly with the software MatCalc.

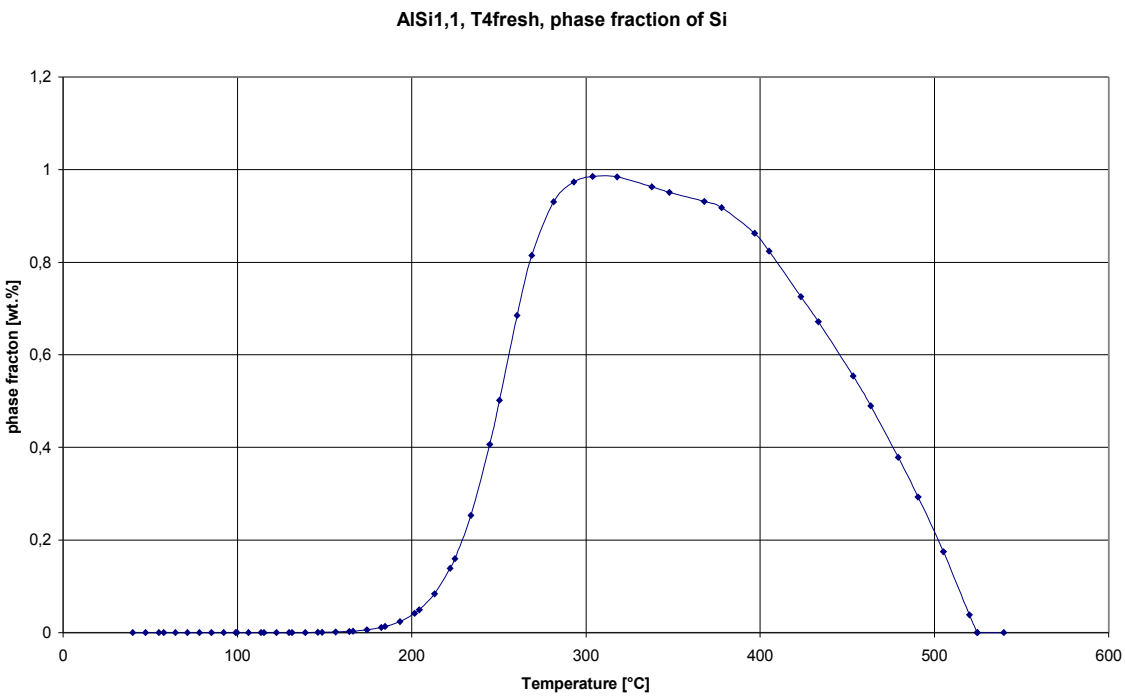

figure 22: Phase fraction of Silicon is Al-Si 1,1 T4fresh, during heating up at 5K/min

The result presented in figure 23 is the MatCalc simulation. The computation will be carried out in following stated sequence. At first considering a T4 fresh condition, the computation of precipitation kinetics with 5 K/min heating rate is performed, the physical database is loaded, molar volume of the considered system is plotted. Numerical derivative of molar volume of the system with respect to temperature is taken and is multiplied by a constant unit conversion factor to convert it to ppm/K.

Compared to the experimental results, the simulation of CTE with MatCalc leads to a precipitation peak of silicon at 250 °C which shows the same temperature as the experiment. Whereas the maximum of CTE on experiments is about 37 ppm/K, the maximum of CTE in the MatCalc simulations is about 55ppm/K which is pretty higher than the experiments.

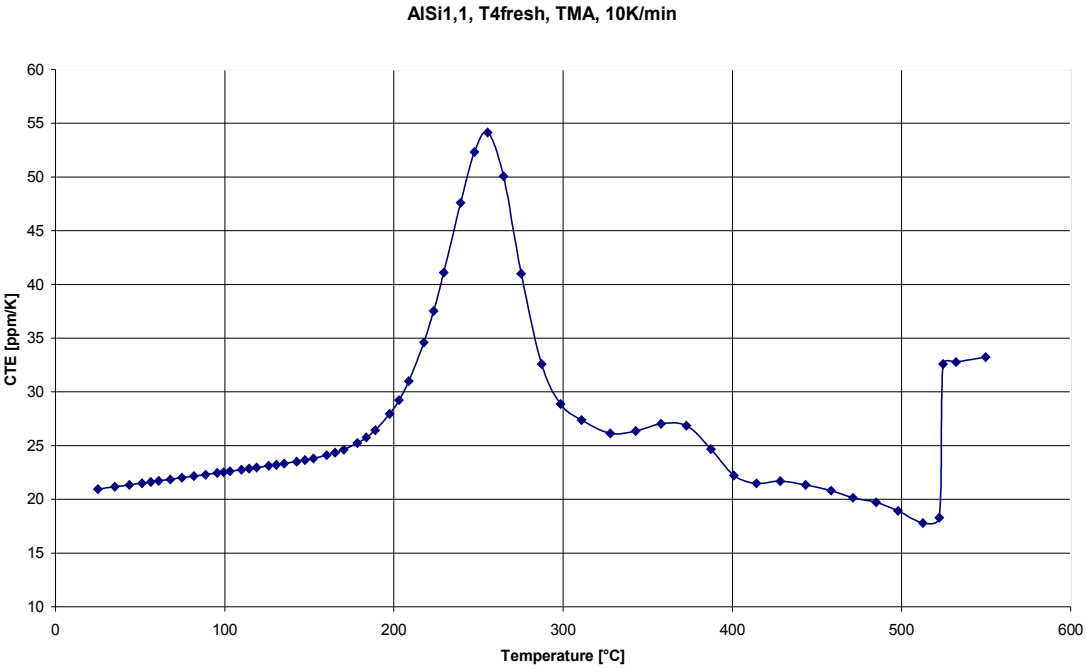

figure 23: Simulation of CTE with MatCalc 5.32 for Al-Si 1,1 wt.% T4_fresh

Using the formulas explained in section 5.3 and partially the results of MatCalc computation, it is possible to perform simulation of CTE for models AA and B2. The results are presented on figure 24 The results of MatCalc computation of CTE is also presented in the same figure.

All these simulations lead to almost similar curves. A large CTE peak of Si precipitation is observed at a temperature range from 200°C to 300°C. The only differences in the simulation results are the height of the peaks and partially dissolution of Si at higher temperatures. Considering more sophisticated models taking in to account matrix composition changes and interaction parameters of elements in matrix etc lead to higher Si precipitation peak.

Although simplified models like A (no matrix composition dependence) or even B2 shows better agreement with experimental results but one should bear in mind that model C is the only comprehensive model. The reason for higher CTE peak values of MatCalc should be investigated.

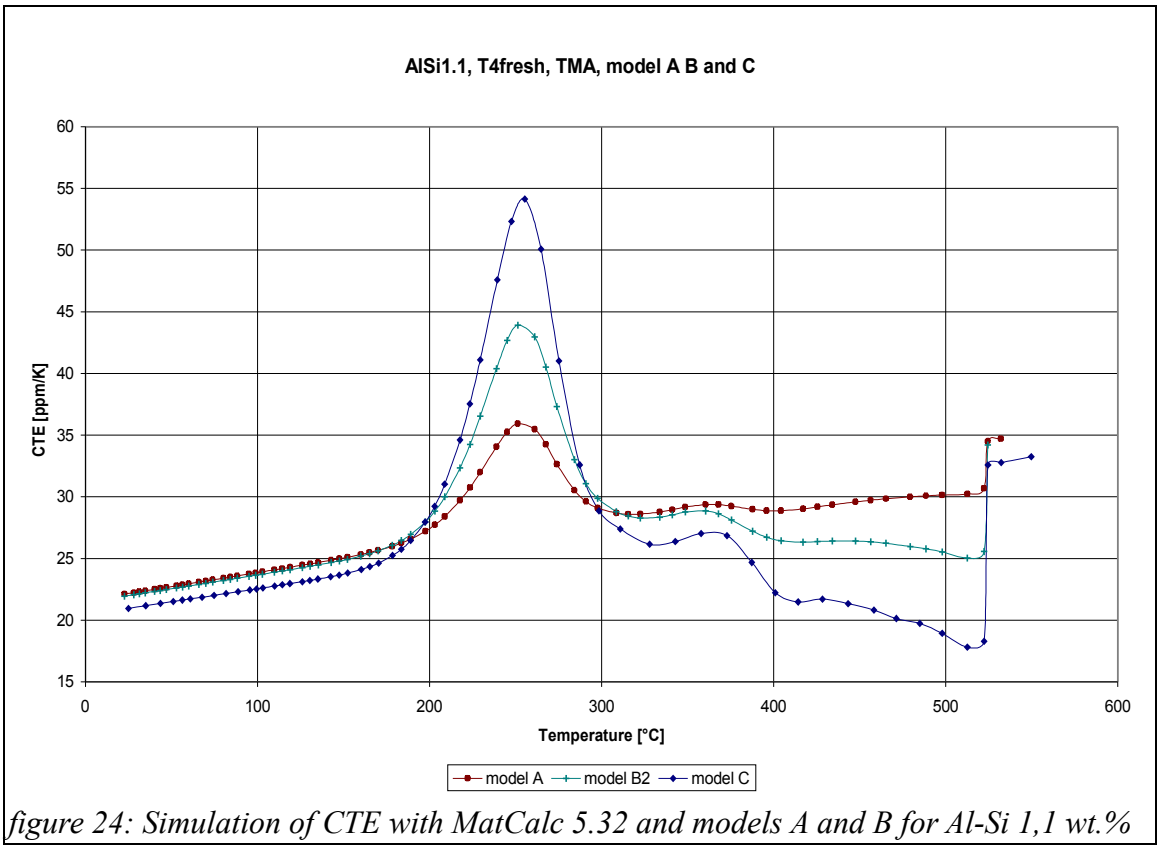

figure 24: Simulation of CTE with MatCalc 5.32 and models A and B for Al-Si 1,1 wt.%

6.3. Aluminium-Magnesium-Silicon AA6016 Alloy

6.3.1. Difference Scaning Calorimetry

Results of DSC scan of AA6016 alloy in the T4_fresh state are presented in curves 25 and 26 . They were tested with two different heating rate: 5K/min for figure 25 and 10 K/min for figures 26. For both heating rates, the same succession of endothermic and exothermic peaks can be observed. The difference consists only in the intensity and the temperature of appearance of these peaks. The focus of this work is not to explain the phenomena which are responsible for these peaks, for more information, one could refer to [21] or [23]

As the shape of these curves is well known, reproducibility of these results was not ensured.

6.3.2. Dilatometry

Material used is AA6016 alloy in the T4_fresh state. Results of TMA experiments are presented in figures 27 and 28. Dilatometry has been carried out with two different heating rates: 5K/min and 10K/min as given in figure 27 and figure 28 respectively. Same succession of peaks can be observed on these curves. Their results are summarised in table 11. Reproducibility was ensured through 2 runs repetition of the experiments.

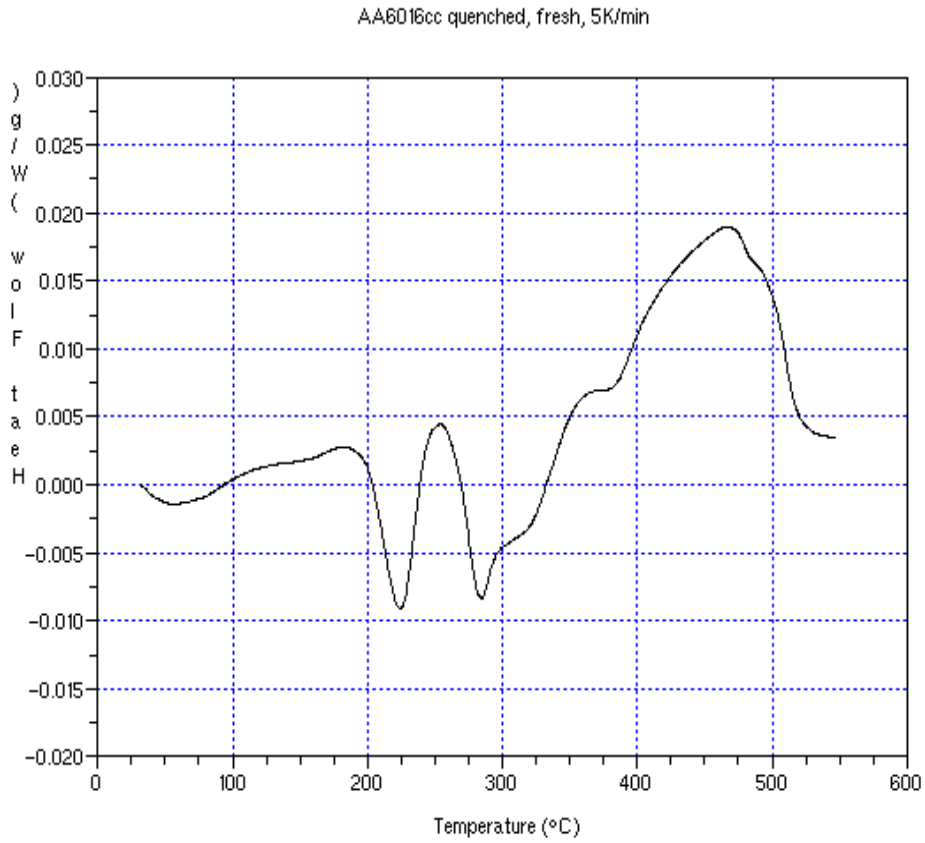

figure 25: DSC results for AA6016, T4_fresh, heated with 5K/min

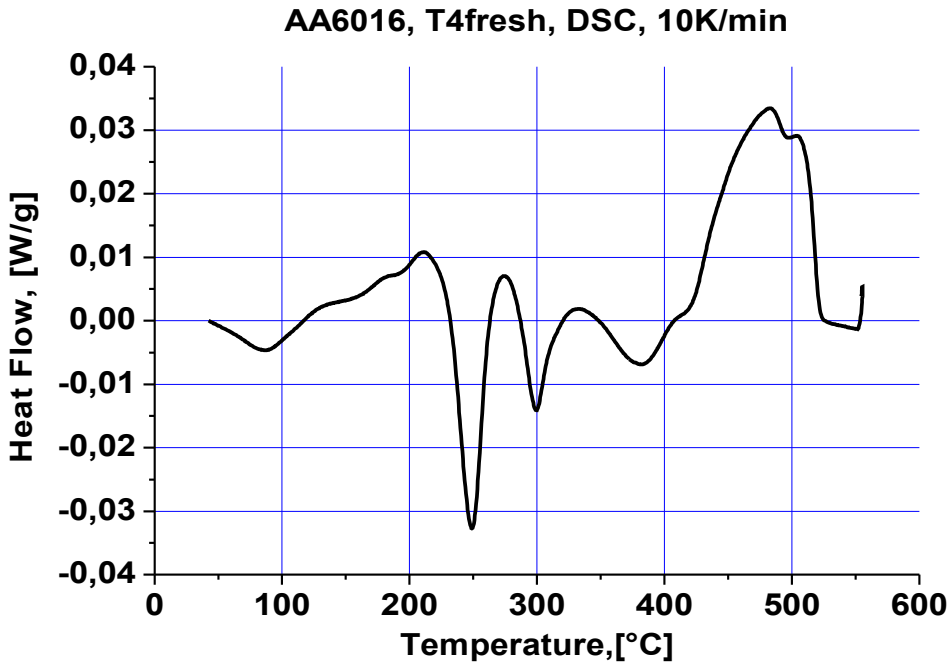

figure 26: DSC results for AA6016, T4_fresh, heated with 10K/min

Table 11: Peaks observed on TMA for A6016 in T4_fresh

Peak No.	direction	Temperature and amplitude Heating rate:5K/min	Temperature and amplitude Heating rate: 10K/min
1	up	220°C (27ppm/K)	250°C (28ppm/K)
2	up	310°C (34 ppm/K)	360°C (33ppm/K)
3	down	450°C (26 ppm/K)	450°C (26 ppm/K)

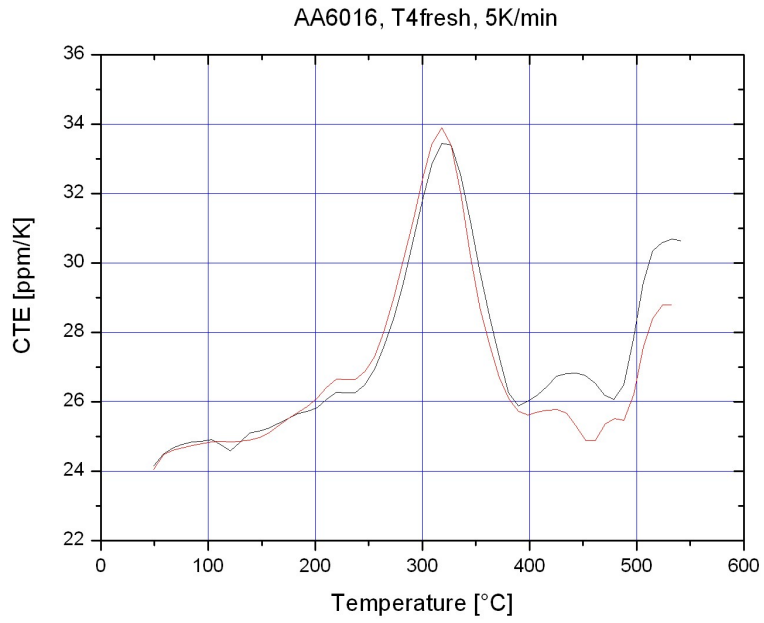

figure 27: TMA results for AA6016, T4_fresh, heated with 5K/min
Legend: 1st run in red and 2nd run in black

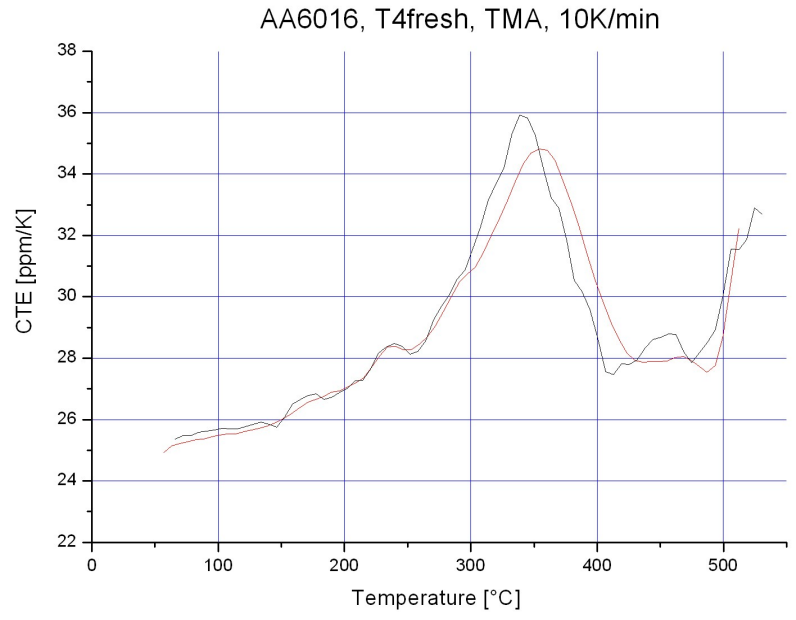

figure 28: TMA results for AA6016, T4_fresh, heated with 10K/min
legend: 1st run in red and 2nd run in black

6.3.3. MatCalc Simulation

The dilatometry behaviour of AA 6016 was simulated with MatCalc 5.41.0.021. The thermodynamic database v1.013 and the diffusion database 1.03 were used. Elements Al, Mg, Si and Vacancy were selected, and the phases FCC_A1, MGSI_CL (clusters), FCC_L12 (GP_Zones), MG5SI6_B_DP (β" precipitate), MGSI_BP (β' precipitate), MG2SI_B (stable β phase) and SI_DIAMOND (stable Si precipitate) were considered as metastable and stable phases involved in kinetics simulation. The weight fraction of Magnesium and Silicon were set respectively to 0.35 wt.% and 1.05 wt.% in order to take into account the Si pick up by Fe and Mn intermetallic phases which will form during solidification and remain almost unchanged during further process or heat treatments.

After precipitation kinetics computation by MatCalc, the physical database 1.009 was loaded and the phase fractions as well as instantaneous CTE were plotted. Phase fractions are presented on figure 29. The prediction of CTE after quenching and heating with a constant heating rate of 5 K/min is presented in figure 30.

In this figure the straight line is the quenching line and because of fast cooling no time is given for precipitation or dissolution. During slow heating of 5 K/min the overall effect of volume changes due to precipitation or dissolution is recognizable on simulation curve as different peaks.

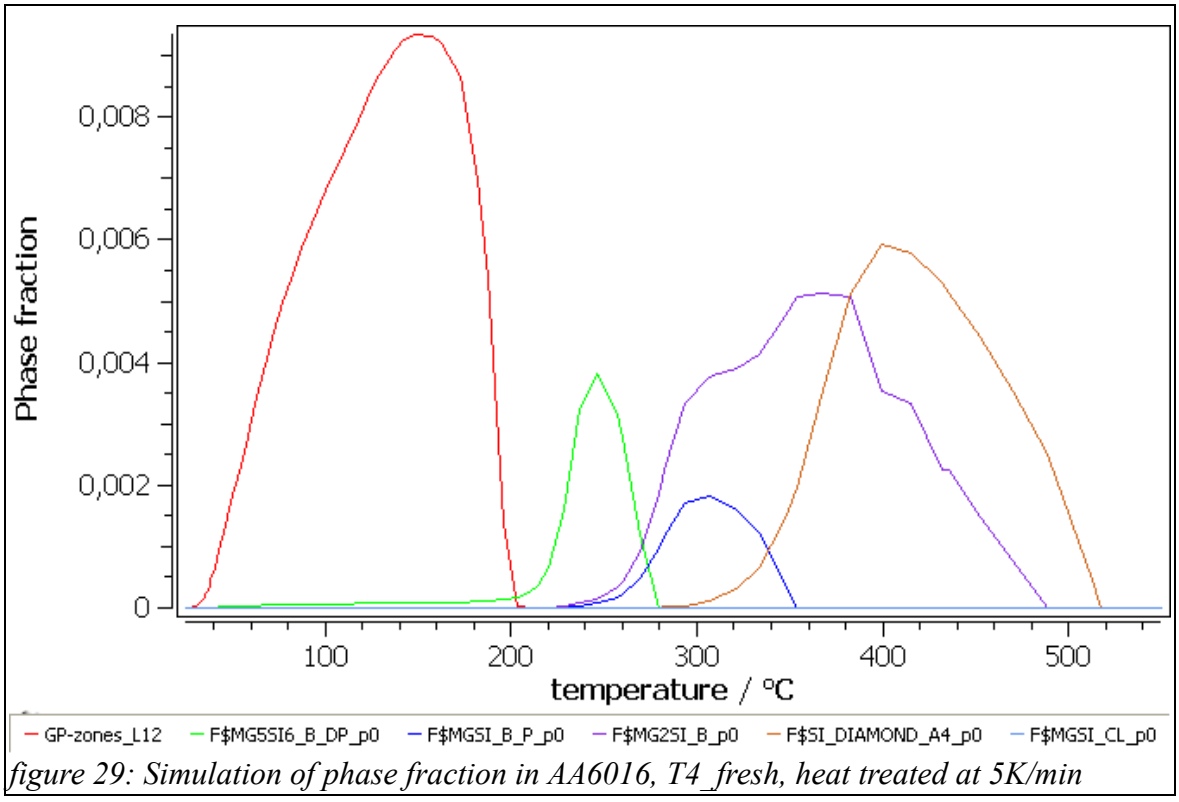

figure 29: Simulation of phase fraction in AA6016, T4_fresh, heat treated at 5K/min

Comparing experimental results (Figure No. 27) with the simulation (Figure No. 31), overall shape of the curve is reproduced. A succession of peaks can be observed. However, major simulation peak is shifted to higher temperature in compare to experimental results.

A comparison of experimental and simulated DSC with the same kinetic parameters as used in dilatometry simulation is shown in figure 32. There is a good correlation of simulation with respect to the experiment. Curves are similar in shape and peak positions. However, the heights of some peaks are higher than experiment.

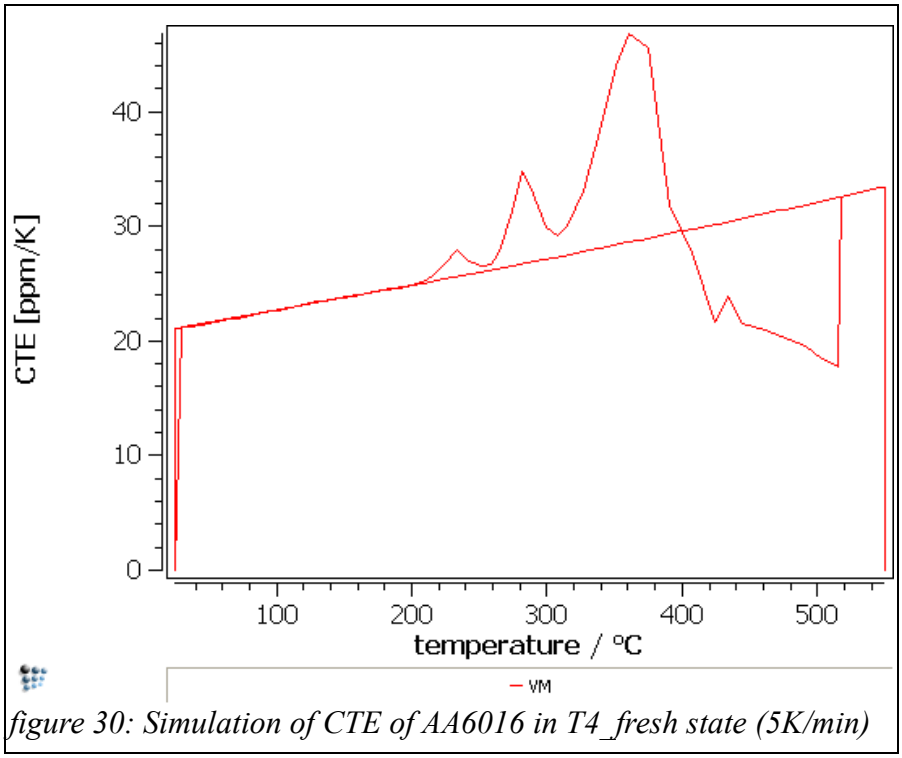

figure 30: Simulation of CTE of AA6016 in T4_fresh state (5K/min)

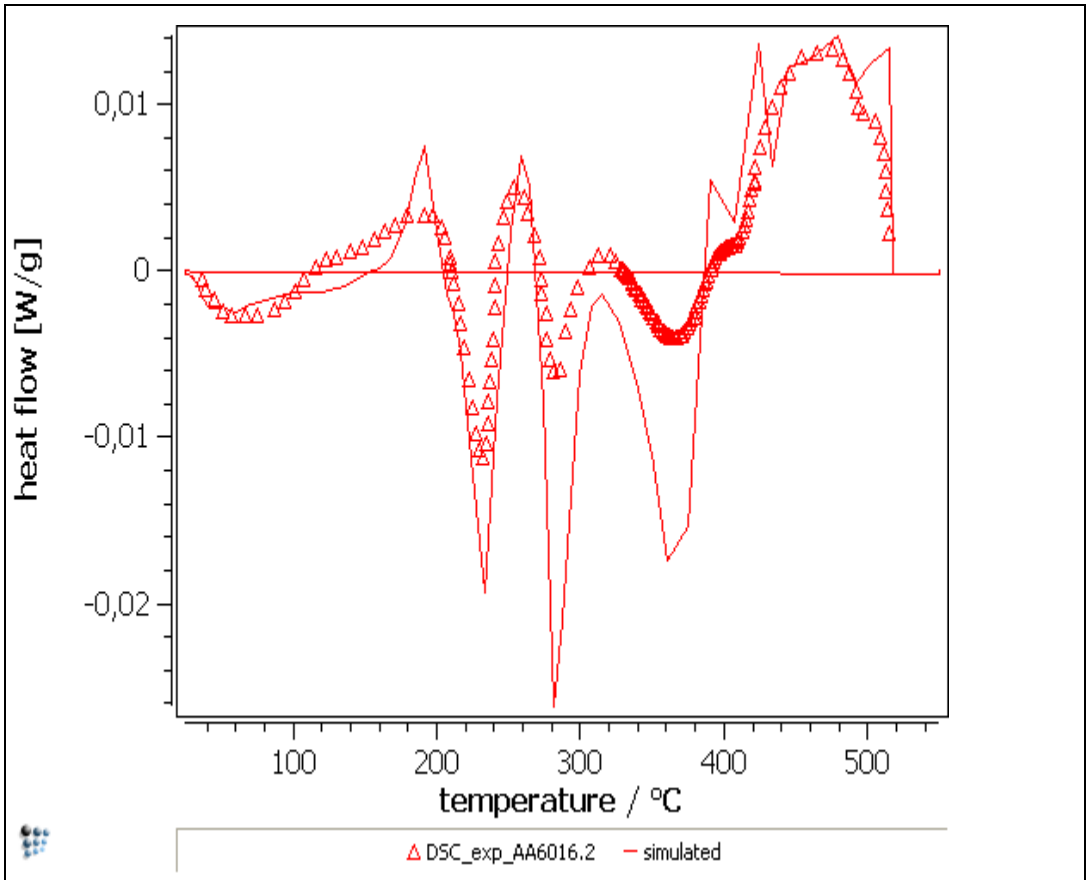

figure 31: A comparison of DSC experiment and simulation of AA6016 in T4_fresh state heating rate : 5K/min

The same kind of simulation can be performed for AA6016 in the T4_fresh state, with a heating rate of 10K/min. Results are presented on figure 32 and 33. Phase fraction which are presented on figure 32 are the result of Matcalc computation with the same databases as previously. From these phase fraction, a prediction of CTE can be computed. Results are presented on figure 33.

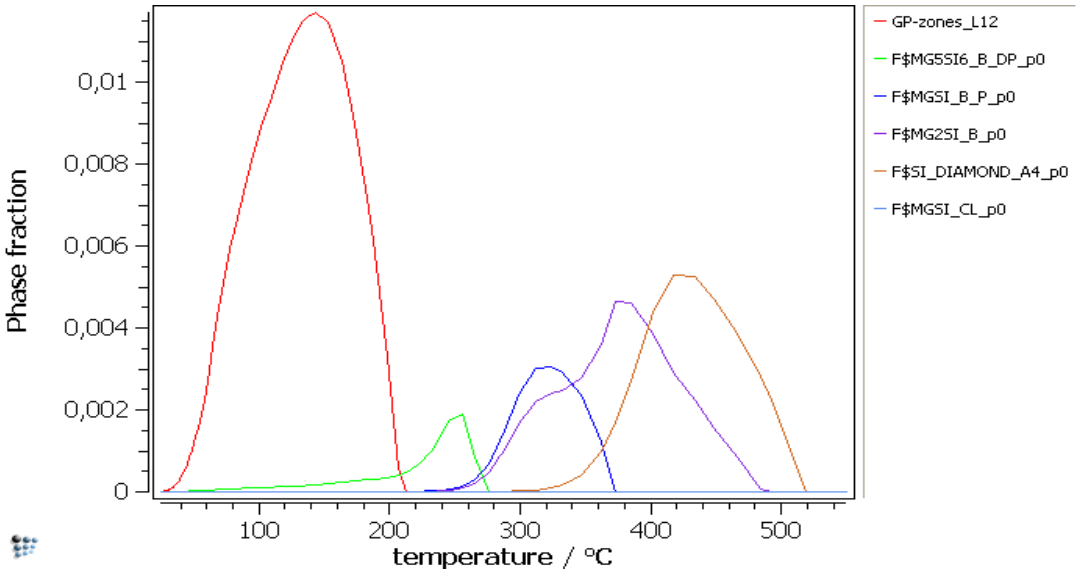

figure 32: Simulation of phase fraction in AA6016, T4_fresh, 10K/min

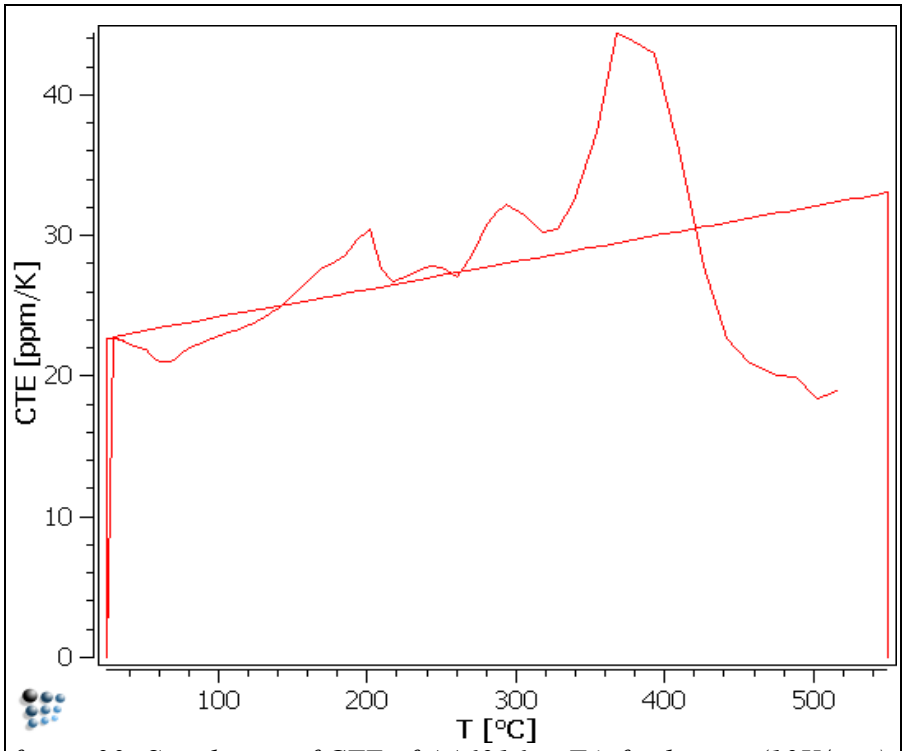

figure 33: Simulation of CTE of AA6016 in T4_fresh state (10K/min)

On this curve, the contraction peak that is formed at very high temperature is a simulation artefact and no attention shall be attributed to it.In this figure the straight line is the quenching line and because of fast cooling no time is given for precipitation

or dissolution. During slow heating of 10 K/min the overall effect of volume changes due to precipitation or dissolution is recognizable on simulation curve as different peaks.

The behavior at low temperature can hardly be compared with experiments, due to the ack of data. However, it seems that MatCalc computations lead to an over-estimation of the inflence of dissolution of GP-Zones, which occurs at about 200°C.

All other peaks seem to be shifted on the right, so on higher temperature. However, this is not correlated with the physical database. Through the adjustment of the simiulation parameters, the curve might be improved. Whenever the height of the peaks is concerned, the peaks seem to be higher than the experimental valued. Maximum peak is reached with more than 40 ppm/K on simulation, whereas the maximum of CTE in experiments is rather about 35 ppm/K.

However, the overall shape of the curve seems to be reproduced.

6.4. Aluminium Copper Alloys

6.4.1. Differential scanning calorimetry

The DSC scan of Al-Cu 4,3 alloys shows a succession of peaks. For this alloy, in the T4_fresh state and a heating rate of 5K/min, the peaks that can be observed are summarised in the table 12. On figure 34, two runs are presented. As can be seen from the results in figure 34 reproducibility of the results is outstanding..

Table 12 : peaks position on Al-Cu 4,3 DSC scan

Peak nr.	Temperature	Orientation
1	60°C	exothermic
2	190°C	endothermic
3	320°C	exothermic
4	400°C	endothermic
5	420°C	exothermic
6	460°C	endothermic

6.4.2. Dilatometry

The CTE plot of the Al-Cu 4.3 in T4_fresh state, with heating rate of 5K/min is presented in figure 35. It has three significant peaks. The first one is a slight dilatation peak, which occurs at about 190°C with an intensity of about 27 ppm/K. The second peak is a large dilatation peak, which reaches a maximum of 38 ppm/K at 300°C. The last peak is a contraction peak, at 400°C with an intensity of 22 ppm/K. As can be seen from the two runs in figure 35, reproducibility has been ensured.

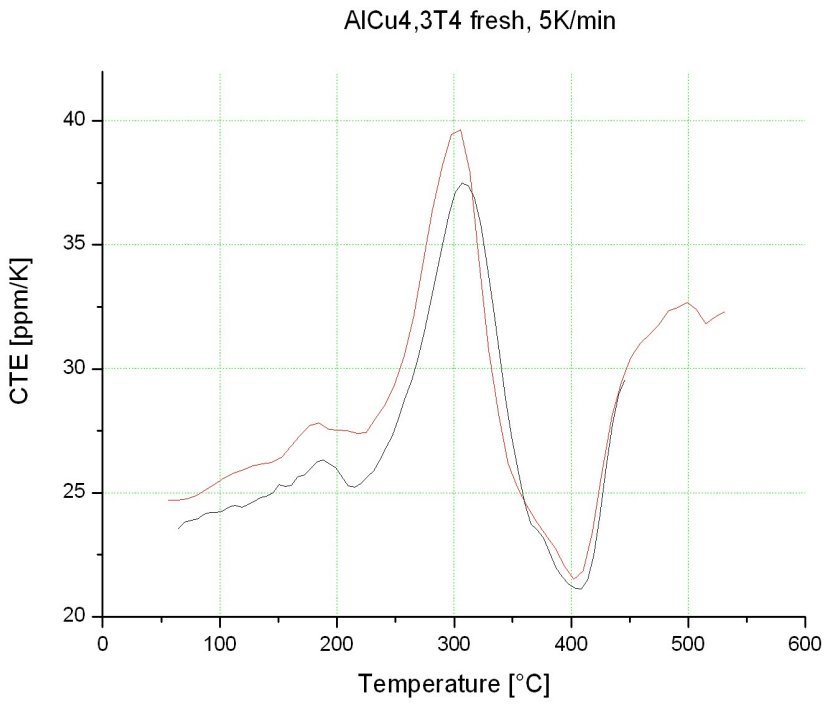

figure 34: TMA experimental result, Al-Cu 4,3, T4fresh, heating 5K/min
Legend: run 1 in red and run 2 in black

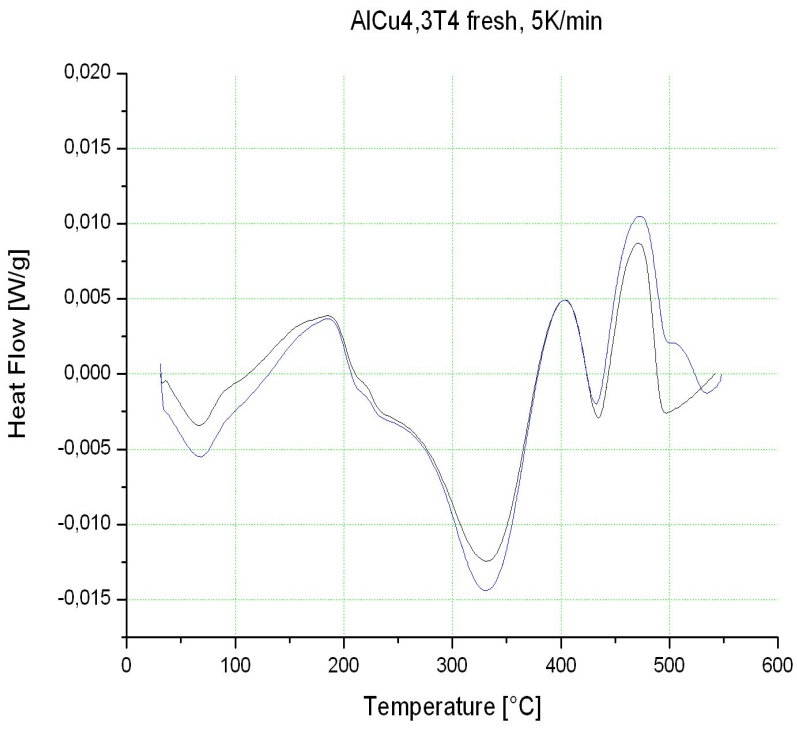

figure 35: DSC experimental result, Al-Cu 4,3, T4fresh, heating 5K/min
Legend: 1st run in blue and 2nd run in black

6.4.3. Results of the MatCalc simulations

Simulation was performed with version 5.41.0.021 of MatCalc. The thermodynamic database version 10, the diffusion database version 3 and the physical database 1.007 were used. Elements Al and Cu and in addition Vacancies were selected. , Considered phases in the simulations are FCC_A1, ALCU_TH_DP (θ”), ALCU_TH_P (θ') and ALCU-THETA (θ) and SI_DIAMOND. The amount of copper was set to 4.3 wt.%.

The MatCalc computes the phase fractions of all phases which are available in the system during the heat treatment process. From this phase fraction data, which are presented on figure 36 one can perform the simulation of CTE directly with MatCalc..

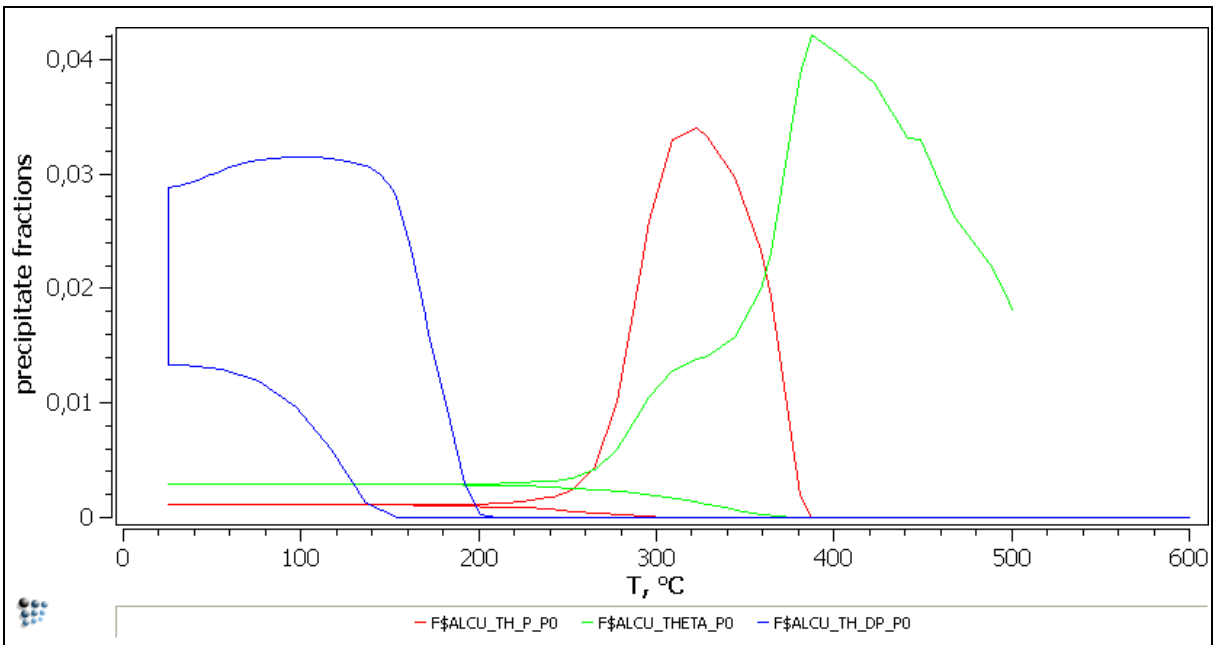

figure 36: simulation of phase fraction in Al-Cu 4,3, T4_fresh during cooling down and further heat treatment at 5K/min

After phase fraction computation is performed, physical database is loaded. The molar volume of the considered system is plotted. One third of derivative of the molar volume of the system with respect to temperature is CTE.

In this plot (see figure 37), three major peaks are observed at 160°C, 290°C and 370°C. The oscillations at high temperatures are numerical simulation artefact.

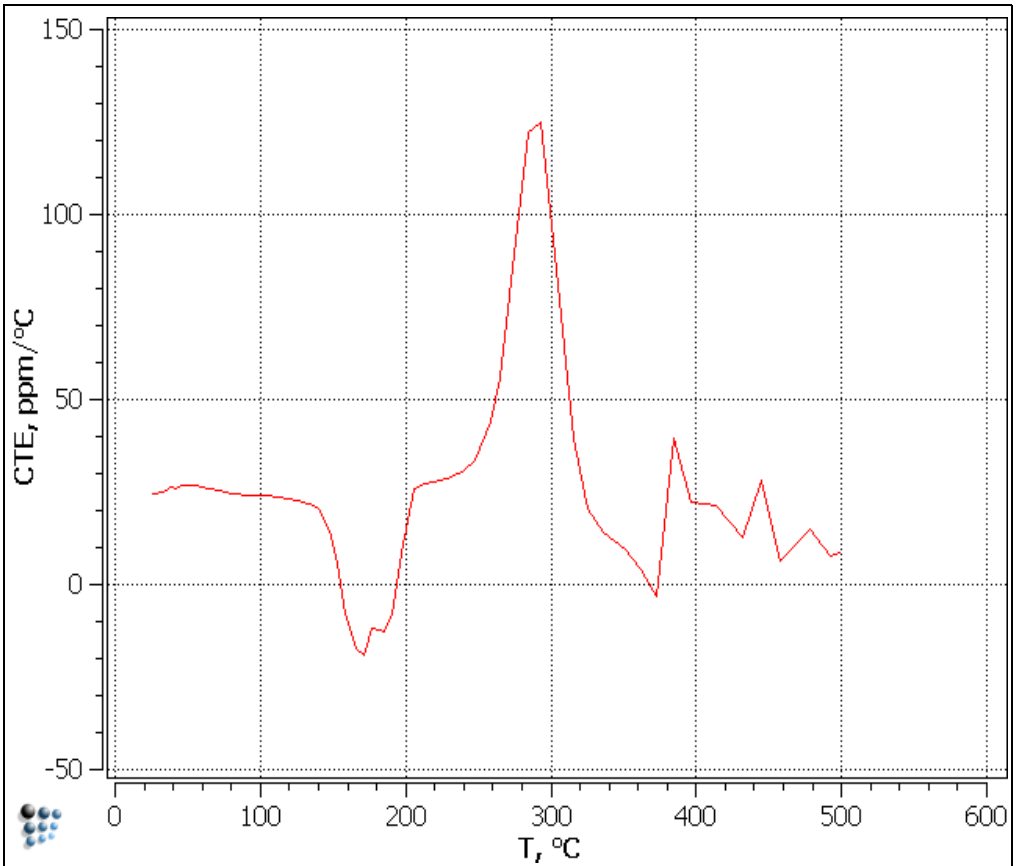

figure 37: CTE prediction by MatCalc for Al-Cu 4,3, T4fresh, heating 5K/min

Compared to the experimental results, the simulation of CTE with MatCalc leads to the same number of major peaks. The sequence of contraction and expansion is also the same. Both show the CTE at 50 °C about 25 ppm/K. But one can see also some differences that have been recognized in other CTE simulation too. This means the peaks are shifted with respect to temperature. Simulation temperature shifts in compare to experiment corresponding to peak 1, 2 and 3 are -30, -10 and -30 °C respectively. Amplitudes of the peaks generally are higher than experimental values.

For compare with DSC experiments, the plotted prediction of heat flow by MatCalc with the same parameter as in CTE simulation is presented in figure 38. The overall shape of the curve predicted matches with the experiment and as the first trial of DSC simulation of AlCu 4.3 is encouraging!

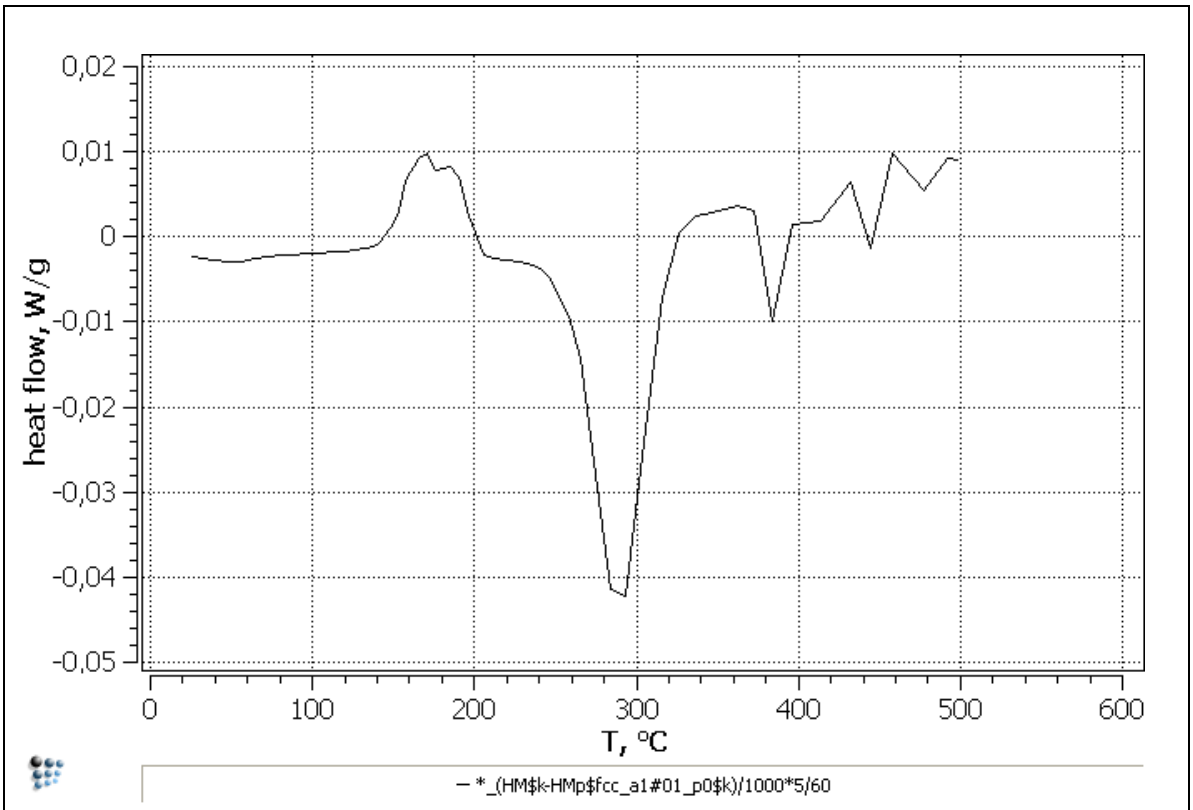

figure 38: DSC prediction by MatCalc for Al-Cu 4,3, T4fresh, heating 5K/min (Same kinetic parameters are used as in dilatometry simulation)

7. Discussion

7.1. Physical database in MatCalc

Physical database in MatCalc is at the heart of volume changes modelling. It takes into account the density of the phases and their temperature dependence, or another way to say their molar volumes as a function of temperature in the calculation. These parameters are important for modelling the volume changes during phase transformation or expansion due to temperature.

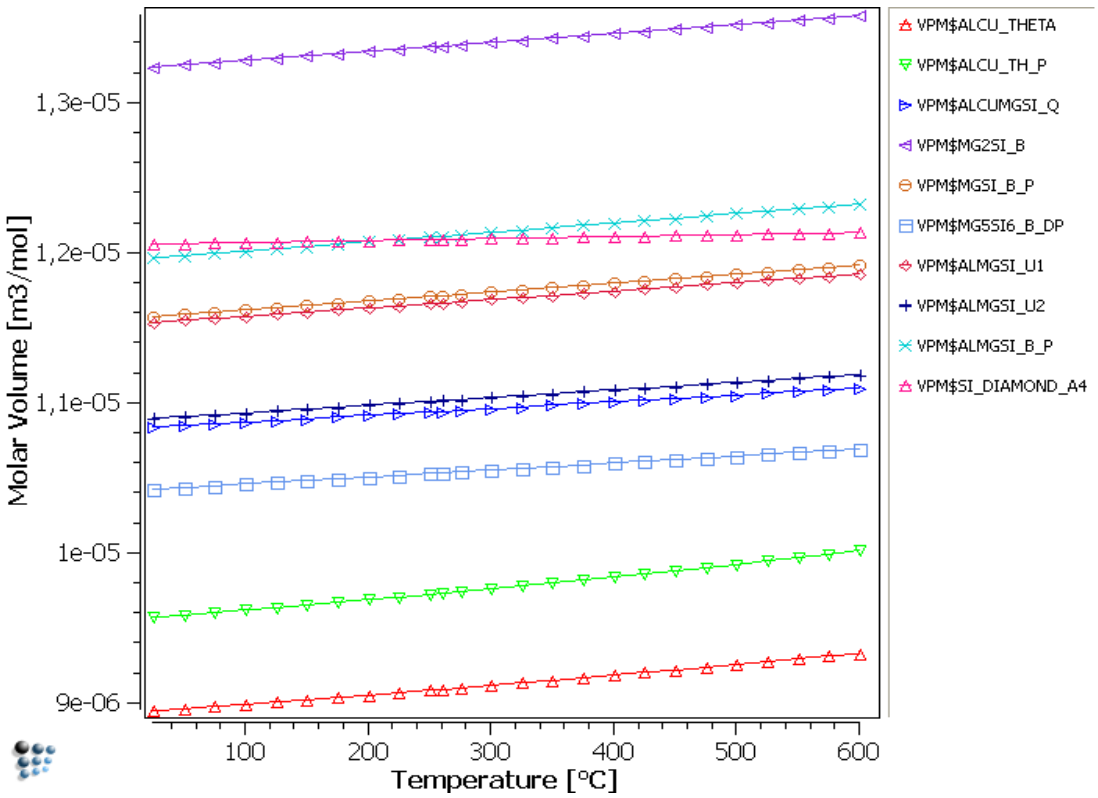

figure 39: Molar Volulmes of the different precipitates of the physical database 1.009

The molar volume of different metastable or stable phases with in the scope of this thesis versus temperature are presented in Figure 39. The difference between the phases is highlighted in the figure. Some phases do appear as having higher molar volume, like the β phase, the silicon diamond-shaped precipitate and the β' phases. These phases (see equation 13) are expected to contribute more pronounced to the volume changes. Some phases, like θ precipitates or θ' precipitates, have lower molar volume in compare to pure aluminium (about 10^{-5} m^3/mol). They are expected to reduce the volume of the alloy when they are formed. Some other precipitates, like the θ" or the GP-Zones have molar volume which are close to pure aluminium. These are expected not to contribute to volume changes.

Experiments seem to bring a good correlation to the above stated expectation. For the Al-Si alloy, precipitation of silicon contributes to an increase of CTE, whereas

dissolution of silicon contributes to a decrease of CTE. For AA6016, depending on temeperature and heat treatment process, several phases precipitate and dissolve at the same time. Precipitates with the highest molar volume difference from the aluminium matrix are β and silicon precipitates. β' also has a high molar volume.

Note: The physical database 1.009 which is presented in appendix 1 has been partially developed from the data collected in table 5.

7.2. Influencing parameters

The models for comparison that has been developed summarise the influencing parameters on the CTE of an alloy. Referring to equation (13), the influencing parameters are the densities of precipitates and their derivatives, the phase fractions and their derivative and the chemical composition of the matrix and its derivative.

Models stated as A and B are less sophisticated and ignore some physical factors involved in compare to MatCalc calculations. However, they are useful in a first approach of modelling and also to recognise the involving parameters in thermal expansion of alloys.

From the compared models, used for Al-Si 1.1 and AA6016, it is possible to highlight that the variation of density of the phases with temperature will have a small contribution to the CTE, whereas the density of precipitates themselves and the changes in matrix compositions and phase fractions will be very important. Comparing dilatometry experiments and their simulations in addition to consideration of phase fraction versus temperature give suitable inputs for improving kinetics simulation parameters.

In the experimental results, phase fractions curves are also presented. They allow comparing the CTE and DSC prediction with the precipitates formedor dissolved at microscale. However, several phenomena can occur at a given CTE-peak. For instance, the large dilatation peak in AA6016 alloys (see figures 29 and 30 or 32 and 33 for compare) can be related to precipitation of the stable phases, but also to dissolution of β' precipitates. Thus a quantitative appreciation of the contribution of the different phases is really a difficult matter, unless the precipitation in the system is simple, like in Al-Si alloys. (see figures 22 and 23 for instance)

In literature, several lattice parameters are often reported for a single structure. For instance, in refernce [30] lattice parameters for β” precipitate are reported deferent from those used in the physical database. However, the difference in terms of density is very slight and this difference is not significant for explaining the deviations between modelling and experiments. Data used for computing thetable 5 are chosen for their coherency between several authors using different methods when possible.

7.3. Correlation to DSC experiments

Both DSC and TMA scans of an alloy bring information about phenomena happening at microscale. The information that is given by these testing methods are of different types: TMA delivers physical information whereas DSC delivers thermodynamics information. Both experiments are important for validation of the models. Inquiries on the possibility to predict heat flow on aluminium samples with MatCalc has been carried out for longer time [32]. Tries to predict the CTE is new. Challenging part in modelling of Al-alloys consist in adjusting simulation parameters to reproduce both curves.

From the physical database and the simulation of heat flow with MatCalc, a first step was achieved in direction of validation and optimising of the model. As one can notice from figures 30 31 and 33 good results are obtained for AA6016. In order to get better results, model has to be improved by taking into account other metastable phases than can coexist along with β' and considering different kinds of GP-Zones in the simulation. Compared to the simultion, in reference [32], the many improvements is already achieved. But this challenge still exists.

7.4 Further perspectives

The methodology that has been used in this work can be used for other systems and other alloys too. Not only alloys in the same category of Al-Mg-Si system considered, such as AA6082 is to be consider, but also Al-Mg or Al-Zn-Mg alloys could be modeled using the same way.

Optimizing the simulation parameters to get correctly DSC and dilatometry with different heating rates is important and is a base for appropriate simulation and predicting the behaviour of any arbitrary alloys with any arbitrary heat treatments.

The question of age hardening is especially important in case of industrial applications. A satisfying modelling that brings more and more precise prediction of the behaviour of different alloys in case of age-hardening is and will remain as an important task for further works.

8. Summary

In this work, the difficulties that can exist to model volume changes during heat treatment in several alloying systems was described and discussed. This approach was a first inquiry for possibility of modelling these phenomena with MatCalc and a progressive approach was adopted, with several systems and several models.

However, a unique way of proceeding was used. An alloying system was chosen and literature review on the involved systems was led out. From this literature review, an understanding of the precipitation phases involved and an assessments of available stereochemical information to update the physical database with density of new phases has been carried out. Experimental results of dilatometry has been compared with MatCalc simulation of the same experiment. DSC experiments and simulations have been carried out as complementary supporting information of dilatometry simulation.

In parallel to using thermokinetics software MatCalc some simplified models were used to show the physical parameters involved in computation of CTE.

Simulation of dilatometry test of pure aluminium as the simplest system has been carried out with very good result. The second system was a more complicated one, the Al-Si system. As a fully described and non controversial system, it was a first step in the simulation of an alloy. Good results for modelling and prediction of CTE has been obtained.

Alloy AA6016 involves much more complex precipitation sequence. However, satisfying results were obtained. Thus the physical database that has been developed and implemented in the scope of this work was useful for computation of CTE. However some small shifts in prediction of dilatomertic peaks were notices. In addition the amplitude of the peaks were bigger than experiment.

The Al-Cu thermodynamic database was under development and the first results showed promising DSC and dilatometry simulations. Although the same sequence of precipitations and number of peaks were obtained by DSC and dilatometry simulation but peak shift and higher amplitude in dilatometry results recognised in the simulations. Optimisation of kinetic parameters still remained to get better results.

Due to existing trend in higher prediction of dilatometry peaks a more detailed theoretical investigation would be helpful. Because mostly important precipitates in Al-alloys are metastable, one of the important feed back in evaluation of relevant databases especially Al-thermodynamic database developed is confrontation of simulations with that of DSC and TMA experiments.

There are good perspectives for further development of this work. This topic was much broadened and there remain many questions to be clarified and by answering these challenging questions to get more precise prediction of precipitation phenomena in Al-alloys.

Literature

[1] **E.Hornbogen, H.Warlimont**, Metallkunde, Springer, Berlin, 1967

[2] **F.Ostermann**, Anwendungstechnologie Aluminium, Springer Verlag, Berlin-Heidelberg, 1998

[3] **M.H. Jacobs**, Precipitation Hardening, TALAT lecture 1204, acts from a lecture, EAA, 1999

[4] **A.Gaber, MA Gaffar, MS Mostafa, E.F. Abo Zeid**, Precipitation kinetics of Al-1.12 Mg2SI – 0,35 Si and Al-1,07 Mg2Si – 0,33 Cu, Journal of alloys and compounds, 429, 2007, pp.167-175

[5] **A. Guinier**, Structure of age-hardened aluminium-copper alloy, Nature, 3595, 1938, pp.569-570

[6] **L.F. Mondolfo**, aluminium alloys structure and properties, Butterwoth, London, 1976

[7] **C.Ravi and C.Wolverton**, First principles study of crystal structure and stability of Al-Mg-Cu-Si precipitates, Acta mater, 52, pp 4213-4227, 2004

[8] **S.J. Andersen, C.D. Marioara**, Structural similarity of the precipitates in the Al-Mg-Si system, sildes from a SINTEF conference, 2007, unpublished.

[9] **A. Hayoune, D. Hamana**, Structural evolution during non-isothermal ageing of a dilute Al–Cu alloy by dilatometric analysis, Journal of Alloys and Compounds 474, 2009, pp. 118–123

[10] **Yongjuan Jing**, *Changrong Li, Zhenmin Du, Fuming Wang, Yuepeng Song*, The thermodynamic analysis of Guinier–Preston zones in aged supersaturated Al–Cu alloys, Computer Coupling of Phase Diagrams and Thermochemistry 32, 2008, pp.164–170

[11] **T.J. Bastow, S. Celotto**, Structure evolution in dilute Al(Cu) alloys observed by ^{63}Cu, NMR, Acta Materialia 51, 2003, pp. 4621–4630

[12] **S.K. Son, M. Takeda, M. Mitome, Y. Bando, T. Endo**, Precipitation behaviour of an Al–Cu alloy during isothermal aging at low temperatures, Materials Letters 59, 2005, pp. 629– 632

[13] **S.Q. Wang, M. Schneider, H.Q. Ye, G. Gottstein**, First-principles study of the formation of Guinier–Preston zones in Al–Cu alloys, Scripta Materialia 51, 2004, pp.665–669

[14] **Chao Jiang**, theoretical studies of aluminum and aluminide Alloys using calphad and first-principles approach, PhD Thesis under supervision of Pr.Zi-Kui Liu, Pennsylvanian State University, 2004

[15] **D.J. Chakrabarti, D. E. Laughlin**, Phase relations and precipitation in Al–Mg–Si alloys with Cu additions, Progress in Materials Science 49, 2004, 389–410

[16] **H.R. Mohammadian**, Precipitation kinetics in Al-aloys observed by dilatometry, Ph.D. Thesis under supervision of Pr. Dr. Koweschnik, TU Wien, 2009

[17] **M.A. Gaffar, A. Gaber, M.S. Mostafa, E.F. Abo Zeid**, The effect of Cu addition on the thermoelectric power and electrical resistivity of Al–Mg–Si balanced alloy: A correlation study, Materials Science and Engineering A 465, 2007, pp. 274–282

[18] **M. Murayama, K. Hono**, Pre-precipitate clusters and precipitation processes in Al-Mg-Si alloys, Acta Materialia, vol. 47, nr. 5, 1999, pp. 1537-1548

[19] **W.F.Miao, D.E.Laughlin**, Precipitation hardening in Aluminium alloys 6022, Scripta Materialia, vol. 40, nr 7, 1999, pp. 873-878

[20] **R.Vissers, M.A. van Huis, J.Jansen, H.W. Zandbergen, C.D. Marioara, S.J. Andersen**, The crystal structure of β' phase in Al-Mg-Si alloys, Acta Materialia, 55, 2007, pp. 3815-3823

[21] **K. Matsuda, S. Ikeno, H. Matsui, T. Sato, K. Terayama, Y. Uetani**, Comparison of Precipitates between excess Si-Type and balanced Type Al-Mg-Si Alloys during Continuous heating, Metallurgical and Materials Transactions, 36A, August 2005-2007

[22] **M.A. van Huis, J.H. Chen, M.H.F. Sluiter, H.W. Zandbergen**, Phase stability and structural features of matrix-embedded hardening precipitates in Al–Mg–Si alloys in the early stages of evolution, Acta Materialia 55, 2007, pp. 2183–2199

[23] **A.K. Gupta, D.J. Llyod, S.A. Court**, Precipitation hardening in Al-Mg-Si alloys with and without excess Silicon, Material Science and Engineering, A316, 2001, pp.11-17

[24], **A. Perovic, D.D. Perovic, G.C. Weatherly, D.J. Lloyd**, Precipitation in aluminium alloys AA6111 and AA6016, Scripta materialia, vol. 41, no7, 1999, pp.703-708

[25] **G.A. Edwards, K. Stiller, G.L. Dunlop, M.J. Couper**, The precipitation sequence in Al-Mg-Si alloys, Acta Materialia, no 11, vol 46,, 1998, pp. 3893-3904

[26] **B. Raeisinia, W.J. Poole, D.J. Lloyd,** Examination of precipitation in the aluminum alloy AA6111 using electrical resistivity measurements, Materials Science and Engineering A 420, 2006, pp.245–249

[28] **C.D. Marioara, S.J. Andersen, J. Jansen, H.W. Zandbergen**, The influence of temperature and storage time at RT on nucleation of the β“ phase in a 6082 Al–Mg–Si alloy, Acta Materialia 51, 2003, pp.789–796

[29] **M.A. van Huis, J.H. Chen, H.W. Zandbergen, M.H.F. Sluiter**, Phase stability and structural relations of nanometer-sized, matrix-embedded precipitate phases in Al–Mg–Si alloys in the late stages of evolution, Acta Materialia 54, 2006, pp. 2945–2955

[30] **C. Wolverton**, crystal structure and stability of complex Precipitate phases in Al–Cu–Mg–(Si) and Al–Zn–Mg Alloys, Acta mater. 49, 2001, pp.3129–3142

[31] **E.Kozeschnik**, Thermodynamics and kinetic simulation with Matcalc, lectures notes, Vienna, August 2009, unpublished.

[32] **P. Lang, A. Falahati, E. Povoden-Karadeniz, O. Nodin, P. Warczok, M.R. Ahmadi, E. Kozeschnik**, Simulation of precipitation sequences of metastable and stable phases in Al-Mg-Si alloys, lecture at the Junior Scientist Conference, Vienna 2010.

[33] Kunststoffprüfung, edited by W. Grellmann and S.Seidler, Carl Hanser Verlag, München, 2005.

[34] **B.Hallstedt**, Molar volumes of Al, Li, Mg and Si, Computer Coupling of Phase Diagrams and Thermochemistry 31, 2007, pp.292–302

[35] **V.Lubarda**, on the effective parameter of binary alloys, mechanics of materials, nr35, pp.53-68, 2003

[36] **V.A. Lubarda and O.Richmond**, Second-order elastic analysis of dilute distribution of spherical inclusions, Mechanics of Materials 31, 1999, pp1-8

[37] **D.Gratias**, Introduction a la physique des materiaux, script from the lecture of the Ecole Poytechnique, non edited.

[38] **Y.Le Bouar, J-C. Toledano**, Base physique de la plasticite des solides, script from the the lecture given at the Ecole Polytechnique, Palaiseau, France, non edited

[39] **D. Hamana, L. Baziz, M. Bouchear**, Kinetics and mechanism of formation and transformation of metastable β'-phase in Al-Mg alloys, Materials chemistry and physics, 84, 2004, pp. 112-119.

Figures

Appendix 1: physical database 1.009 (extract)

Due to copyright restriction, the whole database could not be reproduced. This appendix summarises the contribution achieved in the scope of the present work.

```
$ mc_al_v1.009_2010-07-20.pdb
[...]
$ densities at reference T 298 K
$**********************************************************************
*
$
$ density of pure elements at 298 K
FUNCTION D0FCC_AL     2.98150E+02   2698.15; 6.00000E+03   N REF 16    !
[...]
FUNCTION D0FCC_MG     2.98150E+02   1774.83; 6.00000E+03   N REF 15    !
[...]
FUNCTION D0DIAM_SI    2.98150E+02   2329.05; 6.00000E+03   N REF 18    !
FUNCTION D0FCC_SI     2.98150E+02   3060.10; 6.00000E+03   N REF 15    !
[...]$
$Density of intermetallics at 298K
FUNCTION D0_MG2SI     2.98150E+02    1930.0; 6.00000E+03   N REF 21    !
FUNCTION D0_MG5SI6    2.98150E+02    2530.0; 6.00000E+03   N REF 21    !
FUNCTION D0_BP        2.98150E+02    2217.0; 6.00000E+03   N REF on    !
FUNCTION D0_L10GP     2.98150E+02    2678.2; 6.00000E+03   N REF epk10 !
FUNCTION D0_L12GP     2.98150E+02    2678.2; 6.00000E+03   N REF on    !
FUNCTION D0_U1        2.98150E+02    2331.7; 6.00000E+03   N REF on    !
FUNCTION D0_U2        2.98150E+02    2428.9; 6.00000E+03   N REF on    !
FUNCTION D0_BDASH     2.98150E+02    2183.6; 6.00000E+03   N REF on    !
FUNCTION D0_THP       2.98150E+02    4093.4; 6.00000E+03   N REF on    !
FUNCTION D0_THDP      2.98150E+02      3830; 6.00000E+03   N REF epk10 !
FUNCTION D0_TH        2.98150E+02    4377.2; 6.00000E+03   N REF on    !
FUNCTION D0_Q         2.98150E+02    2739.4; 6.00000E+03   N REF on    !
$[...]
$ ######################################################################
$            Delta of densities (d(T)-d(T0) as functions of temperature
$ ######################################################################
$
FUNCTION DTALFCC  2.98150E+02  +46.34733-0.132992*T-0.00007778*T**2;
6.00000E+03   N REF 15 !
[...]
FUNCTION DTMGFCC  2.98150E+02  +38.3462-0.11304*T-0.00005247*T**2;
6.0000E+03 N REF 15 !
[...]
FUNCTION DTMG2SI  2.98150E+02  +26.625-0.0867*T+0.0000018*T**2; 6.00000E+03
N REF epk09 !
FUNCTION DTMG5SI6 2.98150E+02  +33.248-0.1136*T+0.000002367*T**2;
6.00000E+03   N REF epk09 !
[...]
FUNCTION DTSIFCC  2.98150E+02  +734.063765-0.030514*T-0.000011497*T**2;
6.00000E+03   N REF 15 !
[...]
$ **********************************************************************
$ phase FCC_A1
$
$ individuals
PARAMETER DP(FCC_A1,AL:VA) 2.98150E+02           D0FCC_AL+DTALFCC;
6.00000E+03   N !
```

```
[...]
$ Al-Mg-Si system: interactions, regarding to the new end members FCCMG and
FCCSI, a la louche [by on]
PARAMETER DP(FCC_A1,AL,SI:VA;0) 2.98150E+02       -250;   6.00000E+03   N
REF on !
PARAMETER DP(FCC_A1,AL,MG:VA;0) 2.98150E+02       -300;   6.00000E+03   N
REF on !
[...]
$ default
PARAMETER DP(FCC_A1,*)    2.98150E+02            D0FCC_AL+DTALFCC;
6.00000E+03   N !
$
$ ***************************************************************************
$ phase SI_DIAMOND_A4
$
PARAMETER DP(SI_DIAMOND_A4,SI) 2.98150E+02       D0DIAM_SI+DTSIDIAM;
6.00000E+03   N !
[...]
$
$ ***************************************************************************
$ phase MG2SI_BETA
$
PARAMETER DP(MG2SI_B,MG:SI) 2.98150E+02  D0_MG2SI+DTMG2SI; 6.00000E+03
epk09 !
$
$ ***************************************************************************
$ phase MG5SI6_B_DP
$
PARAMETER DP(MG5SI6_B_DP,MG:SI) 2.98150E+02  D0_MG5SI6+DTMG5SI6;
6.00000E+03   epk09 !
$
$ ***************************************************************************
$ phase MGSI_B_P
$
PARAMETER DP(MGSI_B_P,MG:SI) 2.98150E+02  D0_BP+DTMG5SI6; 6.00000E+03
on10+epk10 !
$
$ ***************************************************************************
$ phase ordered GP-zones (epk09)
$
$ "Matsuda model" Al6MgSi (on10)
PARAMETER DP(fcc_L12,*:*:*:*:VA) 2.98150E+02  D0_L12GP+DTALFCC; 6.00000E+03
on10 !
$ "Matsuda model" Al2MgSi (on10)
PARAMETER DP(fcc_L10,*:*:*:*:VA) 2.98150E+02  D0_L10GP+DTALFCC; 6.00000E+03
epk10 !
$
$ ***************************************************************************
$ "Van Huis"-phase Beta_Double_Prime "Initial" (epk)
$
$ Al6Mg2Si3
PARAMETER DP(B_DP_INI,AL:MG:SI) 2.98150E+02  D0_L12GP+DTALFCC; 6.00000E+03
epk10 !
$
$***************************************************************************
*
$ phase ALMGSI_U1
$
$ Al2MgSi2
PARAMETER DP(ALMGSI_U1,AL:MG:SI) 2.98150E+02  D0_U1+DTMG5SI6; 6.00000E+03
on10 !
$
```

```
$ ************************************************************************
$ phase ALMGSI_U2
$
$ AlMgSi
PARAMETER DP(ALMGSI_U2,AL:MG:SI) 2.98150E+02  D0_U2+DTMG5SI6; 6.00000E+03
on10 !
$
$ ************************************************************************
$ phase ALMGSI_B'
$
 PARAMETER DP(ALMGSI_B_P,AL:MG:SI) 2.98150E+02  D0_BDASH+DTMG5SI6;
6.00000E+03   on10 !
$
$ ************************************************************************
$ phase ALCUMGSI_Q
$
 PARAMETER DP(ALCUMGSI_Q,AL:CU:MG:SI) 2.98150E+02  D0_Q+DTMG5SI6;
6.00000E+03   on10 !
$
$ ************************************************************************
$ phase ALCU_TH_DP, earliest GP
$
PARAMETER DP(ALCU_TH_DP,AL:CU) 2.98150E+02  D0_THDP+DTALFCC; 6.00000E+03
epk10 !
$
$ ************************************************************************
$ phase ALCU_TH_P
$
PARAMETER DP(ALCU_TH_P,AL:CU) 2.98150E+02  D0_THP+DTALFCC; 6.00000E+03
epk10 !
$
$ ************************************************************************
$ phase ALCU_THETA
$
PARAMETER DP(ALCU_THETA,AL:CU) 2.98150E+02  D0_TH+DTALFCC; 6.00000E+03
on10+epk10 !
PARAMETER DP(ALCU_THETA,AL:AL) 2.98150E+02  D0_TH+DTALFCC; 6.00000E+03
on10+epk10 !
$
$************************************************************************
[...]
```